Evolution of the margin of the Gulf of California near Loreto, Baja California Peninsula, Mexico

Paul J. Umhoefer*
Department of Geology, Northern Arizona University, Flagstaff, Arizona 86011, USA

Larry Mayer
Department of Geosciences, University of Arizona, Tucson, Arizona 85721, USA

Rebecca J. Dorsey
Department of Geological Sciences, University of Oregon, Eugene, Oregon 97403, USA

ABSTRACT

The Gulf of California is a prime example of a young oblique-divergent plate boundary. This type of plate boundary is much less well understood than classic rifts and passive margins in divergent plate settings. A complexity in the Gulf of California is that the modern oblique rifting was preceded by a stage of orthogonal rifting. We have used extensive mapping as well as stratigraphic, geomorphic, and structural analysis to determine the history of deformation near Loreto on the southern Baja California peninsula during formation of the Gulf of California. Our data support the suggestion that middle to late Miocene (protogulf stage, 12 to ca. 6 Ma) orthogonal rifting was overprinted by transtensional structures during Pliocene to Quaternary time, though we cannot closely define the time of change. We further demonstrate that the plate margin was structurally segmented in the protogulf stage and then complexly overprinted by transtensional structures that suggest one type of process for initiating transform faults.

The Loreto segment is 85 km long along the rift and is bounded on the west by a discontinuous series of aligned, down-to-the-east extensional monoclines and normal faults. These structures lie along, or as far as 4 km in front (east) of, a steep, 1000–1600-m-high Main Gulf Escarpment that defines the western topographic margin of the rift zone. The Loreto segment is further defined by a rise in elevation of the Main Gulf Escarpment of up to 1 km and an ~500–800 m increase in structural relief of prerift strata in the escarpment from the segment boundaries to the center of the segment. Structural analysis of secondary faults of the Loreto segment shows that fault populations that are known to be Pliocene to Quaternary in age are mixed normal and dextral-normal faults with a bulk extension direction of west-northwest–east-southeast (280°–100°). In contrast, fault populations that cut only prerift, Oligocene–middle Miocene volcanic and sedimentary rocks are mainly normal faults with northeast-southwest to east-northeast–west-southwest bulk extension directions that average 245°–65°. These faults are interpreted to be late Miocene in age and formed during protogulf orthogonal rifting. Thus, the Pliocene faults record a major change of extension direction of ~35° from latest Miocene to Pliocene time, compatible with the onset of oblique rifting in the Gulf of California. Oblique-divergent overprinting is mainly expressed as the Loreto fault and Loreto basin in the northern part of the segment. The Loreto fault and basin evolved with major fault reorganizations and partial basin inversion. Many observations suggest that the Pliocene Loreto fault was linked to two nascent transform faults in the gulf and that Carmen Island rotated ~35°–40° clockwise within the complex fault system.

Keywords: basins, faults, Gulf of California, Neogene, plate margins, rifting.

INTRODUCTION

The structural and topographic pattern in continental rifts with orthogonal extension is reasonably well known. These rifts are commonly segmented along the rift axis by a series of major normal faults and half grabens with alternating asymmetry (Fig. 1) (Crossley and Crow, 1980; Ebinger et al., 1984; Bosworth, 1985; Rosendahl et al., 1986; Rosendahl, 1987; Colletta et al., 1988; Ebinger et al., 1989b; Morley et al., 1990; Chapin and Cather, 1994; Lewis and Baldridge, 1994; Hayward and Ebinger, 1996; Upcott et al., 1996). These half grabens vary in length parallel to the rift from ~20 to 150 km, but are characteristically 50–100 km long (e.g., Hayward and Ebinger, 1996). The length of the segments is a function of the seismogenic thickness and elastic thickness of the crust (Jackson and White, 1989; Scholz and Contreras, 1998). Between the rift segments are complex accommodation or transfer zones, across which the style and orientation of faulting changes (e.g., Ebinger, 1989a; Morley et al., 1990; Mack and Seager, 1995; Faulds and Varga, 1998). In an idealized transfer zone (Lister et al., 1986), near-vertical strike-slip faults accommodate the change in the polarity of extension, whereas in an idealized accommodation zone (Rosendahl, 1987; Faulds and Varga, 1998), the changes in polarity are accomplished by relay systems between segments. The topographic relief along the rift flank is caused by footwall uplift on the rift-bounding faults, isostasy from mass redistribution (e.g., Wernicke and Axen, 1988; Braun and Beaumont, 1989; Weissel and Karner, 1989), lateral conduction of heat away from the rift (e.g., Buck, 1988), or greater thinning of the mantle lithosphere than the crust (e.g., Royden and Keen, 1980; Steckler, 1985). Therefore, the height of the rift flanks is commonly greater behind the centers of the segments than in accommodation zones, where faulting is more widely distributed and not

*E-mail: paul.umhoefer@nau.edu.

GSA Bulletin; July 2002; v. 114; no. 7; p. 849–868; 12 figures.

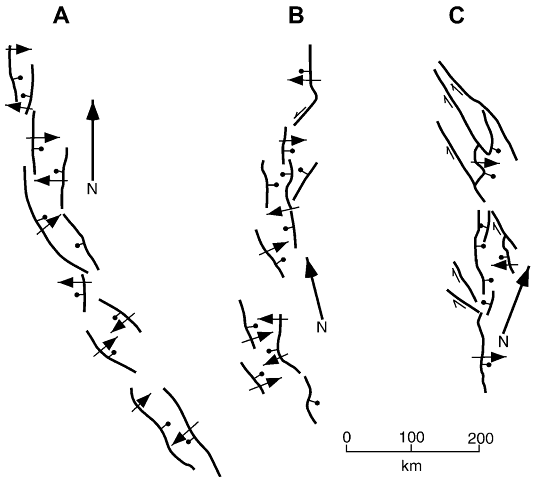

Figure 1. Parts of three major rifts at the same scale. (A) The Tanganyika region of the East African rift after Ebinger (1989b). (B) The Rio Grande rift in New Mexico. (C) The northwestern part of the Gulf of California oblique rift after Axen (1995). Note the similar lengths of the rift segments as defined by the major normal faults (wide lines with stick and ball on hanging-wall side). Also clear is the common alternation of dip direction and symmetry of the normal faults and half grabens and thus the change in the movement of the hanging wall relative to the footwall (as shown by the arrows giving the upper-plate transport direction) along the rifts. The strike-slip faults (shown by small arrows) in C are younger than the rift segmentation.

dominated by one fault (Gawthorpe and Hurst, 1993).

The structural patterns in oblique rifts are poorly understood compared to those in orthogonal rifts. Tamsett (1984) and Fantozzi (1996) have shown convincing evidence that the margins of the Gulf of Aden contain rift segments. Analogue experiments designed to compare the structural evolution of orthogonal and oblique rifts show that oblique rifts are characterized by shorter segmented border faults and that the major rift faults form en echelon arrays parallel to the underlying zone of extension (McClay and Ellis, 1987). On the basis of analogue modeling, McClay and White (1995) proposed that accommodation zones consisting of systems of conjugate extensional faults accommodate the polarity reversals between rift segments in oblique rifts.

The Gulf of California is an active, oblique-divergent plate boundary. Most workers suggest the Gulf of California had an early stage of orthogonal rifting that was overprinted by the modern oblique-divergent plate boundary (e.g., Karig and Jensky, 1972; Stock and Hodges, 1989). Axen (1995) showed that there are three major rift segments in the northeastern part of the Baja California peninsula that alternate in the symmetry of their major normal faults and half grabens (Fig. 1C). He further speculated that the whole western margin of the Gulf of California on the central and southern Baja California peninsula has ~100-km-scale segments that alternate in the symmetry of their major normal faults and half grabens (Fig. 2). However, nowhere along the southern two-thirds of the Baja California peninsula has the model of segmentation and the two-stage rift model for the gulf been tested with detailed field data over an area large enough to define a segment. We have examined the area near Loreto (Fig. 2) to address the following questions: (1) Is the two-stage model for the Gulf of California correct near Loreto? (2) Is rift segmentation in the southern gulf real? (3) If so, when did segmentation occur? (4) How did oblique rifting overprint the early rift structures?

Here, we report on the structural framework of a 120-km-long coastal belt near Loreto on the central part of the Baja California peninsula (Fig. 2) to explore these four questions and oblique-rifting processes more generally. At the first order, the structures and topography in the Loreto coastal belt strongly suggest that the rift margin is segmented; down-to-the-east extensional structures form the rift boundary along the Loreto segment, in contrast to areas to the north and south where these faults are not found (Fig. 3). The Loreto segment is also defined by changes in the Main Gulf Escarpment, which is higher, steeper, and straighter behind the Loreto segment than in areas to the north and south. Our data on the relative timing of faulting suggest that segmentation was established in late Miocene time during the protogulf stage of orthogonal rifting. We further document the overprinting by oblique-rift structures and speculate on how these evolved relative to the main transform–spreading-ridge system. Our data strongly support the two-stage model for rifting of the Gulf of California and confirm the conclusion of Zanchi (1994), who presented a paleostress analysis of the Loreto region. The two-stage nature of this rifted margin results in a more complex margin than many orthogonal rifts. Our study also provides a detailed database for the onshore Baja California peninsula near Loreto from which to investigate the important offshore margins of the plate boundary, where little is known. This paper is based on 1:50 000 mapping of most of the 120-km-long coastal belt near Loreto, structural, stratigraphic, and geomorphic analysis, and mapping at 1:10 000 and 1:20 000 scales of the central half of the segment. This work builds on previous mapping and analysis by McLean (1988), Zanchi (1994), and Bigioggero et al. (1995) and our own work (Umhoefer et al., 1994; Dorsey et al., 1995; Umhoefer and Stone, 1996; Mayer and Vincent, 1999; Dorsey and Umhoefer, 2000).

TECTONIC SETTING

Formation of the Gulf of California

According to most workers, the Gulf of California (Fig. 2A) underwent a two-stage evolution. Orthogonal rifting during a protogulf stage from 12 to 6 Ma in the southern Gulf of California was overprinted from 6 to 0 Ma by the highly oblique–divergent plate boundary of the modern gulf (Moore and Buffington, 1968; Karig and Jensky, 1972; Hausback, 1984; Stock and Hodges, 1989; Lonsdale, 1989; Zanchi, 1994). From ca. 25 to ca. 12 Ma, a simple convergent margin involved eastward subduction of various oceanic plates of the Pacific basin beneath the edge of the North American plate (Hausback, 1984; Stock and Molnar, 1988; Sawlan, 1991; Stock and Lee, 1994). A terrestrial volcanic arc was present along the future Gulf of California during this period (Hausback, 1984; Sawlan, 1991), and extensional faulting occurred behind (east of) the arc on present mainland Mexico (e.g., Henry, 1989). The subduction zone was extinguished in jumps from north to south from 16 to 12 Ma as a transform plate boundary formed on the west side of the future Baja California peninsula (Stock and Lee, 1994). From 12 to ca. 6 Ma, a protogulf stage of rifting was accompanied by one or two marine incursions (Smith, 1991). This rifting was part of regional strain partitioning (Hausback,

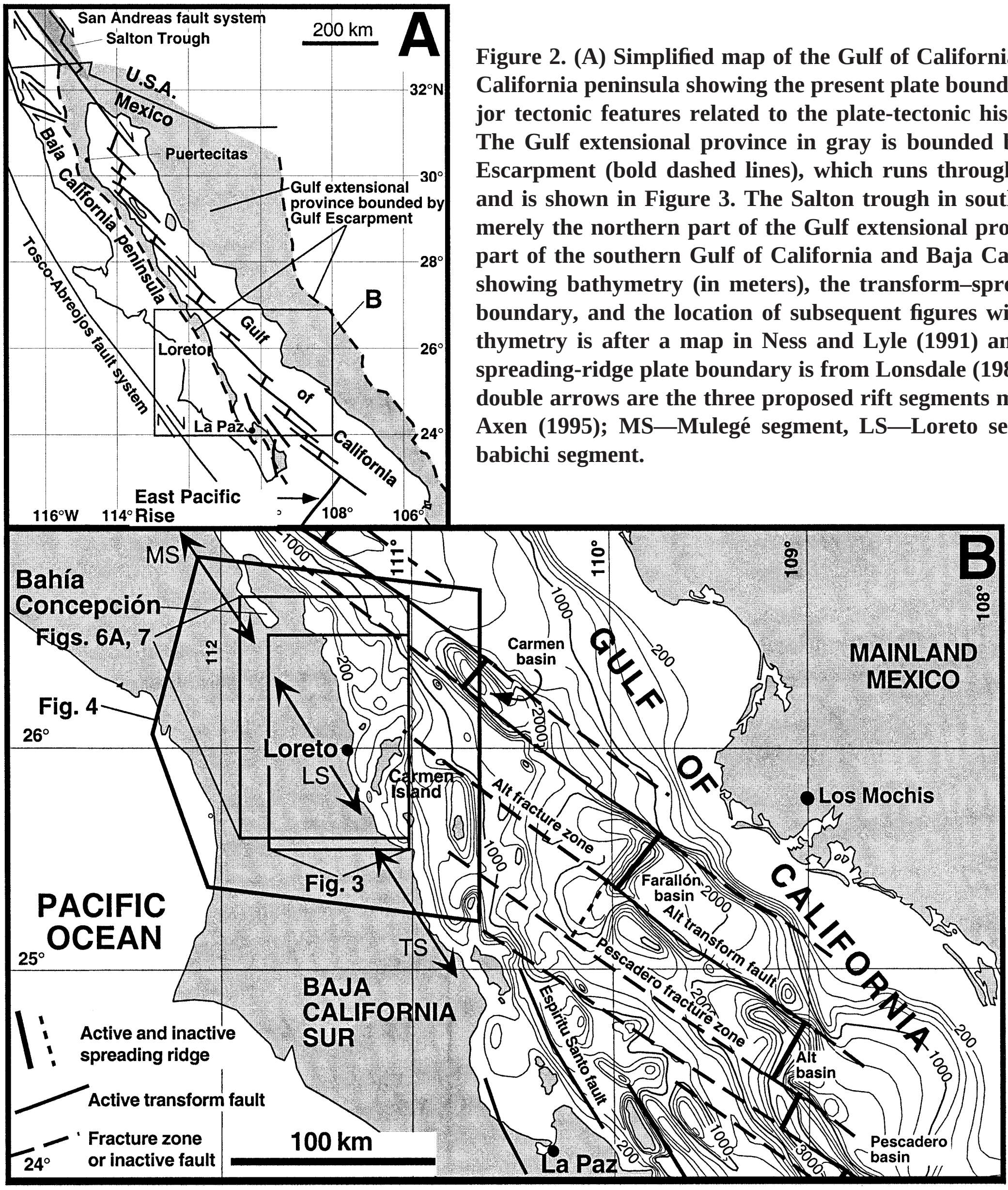

Figure 2. (A) Simplified map of the Gulf of California region and Baja California peninsula showing the present plate boundary and some major tectonic features related to the plate-tectonic history since 12 Ma. The Gulf extensional province in gray is bounded by the Main Gulf Escarpment (bold dashed lines), which runs through the Loreto area and is shown in Figure 3. The Salton trough in southern California is merely the northern part of the Gulf extensional province. (B) Map of part of the southern Gulf of California and Baja California peninsula showing bathymetry (in meters), the transform–spreading-ridge plate boundary, and the location of subsequent figures with maps. The bathymetry is after a map in Ness and Lyle (1991) and the transform–spreading-ridge plate boundary is from Lonsdale (1989). The lines with double arrows are the three proposed rift segments modified here after Axen (1995); MS—Mulegé segment, LS—Loreto segment, TS—Timbabichi segment.

1984; Stock and Hodges, 1989), in which the Tosco-Abreojos transform-fault system lay to the west of Baja California (Fig. 2A) (Spencer and Normark, 1979) and a broad zone of extensional faulting in the region of the present gulf and to the east on mainland Mexico had northeast-southwest to east-northeast–west-southwest extension (e.g., Stock and Hodges, 1989; Henry, 1989). At 6 Ma, the plate boundary started to shift into the Gulf of California and linked to the San Andreas fault system in southern California. This is when the modern system of transform faults and small rift basins was initiated in the gulf (Lonsdale, 1989). However, a recent reanalysis of plate motions suggests that the major change in plate motion off Baja California was at ca. 8 Ma (Atwater and Stock, 1998), and this timing may suggest an earlier change from the protogulf deformation to the later style of deformation. West of Loreto, this change was from Pacific–North American plate relative motion along an azimuth of ~315° to an azimuth of ~300°. Many of the specific points of this two-stage model have not been tested, and other models for the evolution of the Gulf of California have been suggested that involve major strike-slip faulting starting earlier than 6 Ma (Humphreys and Weldon, 1991; Lyle and Ness, 1991).

Lonsdale (1989) suggested that there was a transitional period between the two tectonic stages of rifting from ca. 6 to 3.5 Ma. During this interval, the Tosco-Abreojos transform-fault system continued to be active west of Baja California while the first series of strike-slip faults formed in the gulf, making the Baja California peninsula essentially a separate microplate. Lonsdale (1989) suggested that these initial strike-slip faults in the gulf formed parallel to the gulf and were separated by pull-apart basins. At 3.5 Ma, the full plate boundary moved into the gulf for the first time, and over the next million years or so, the current system of transform faults and small spreading ridges formed (Lonsdale, 1989). Evidence from GPS (Global Positioning System) experiments suggests that the Tosco-Abreojos transform-fault system on the west side of the Baja California peninsula is still active at a low rate of faulting (Dixon et al., 2000).

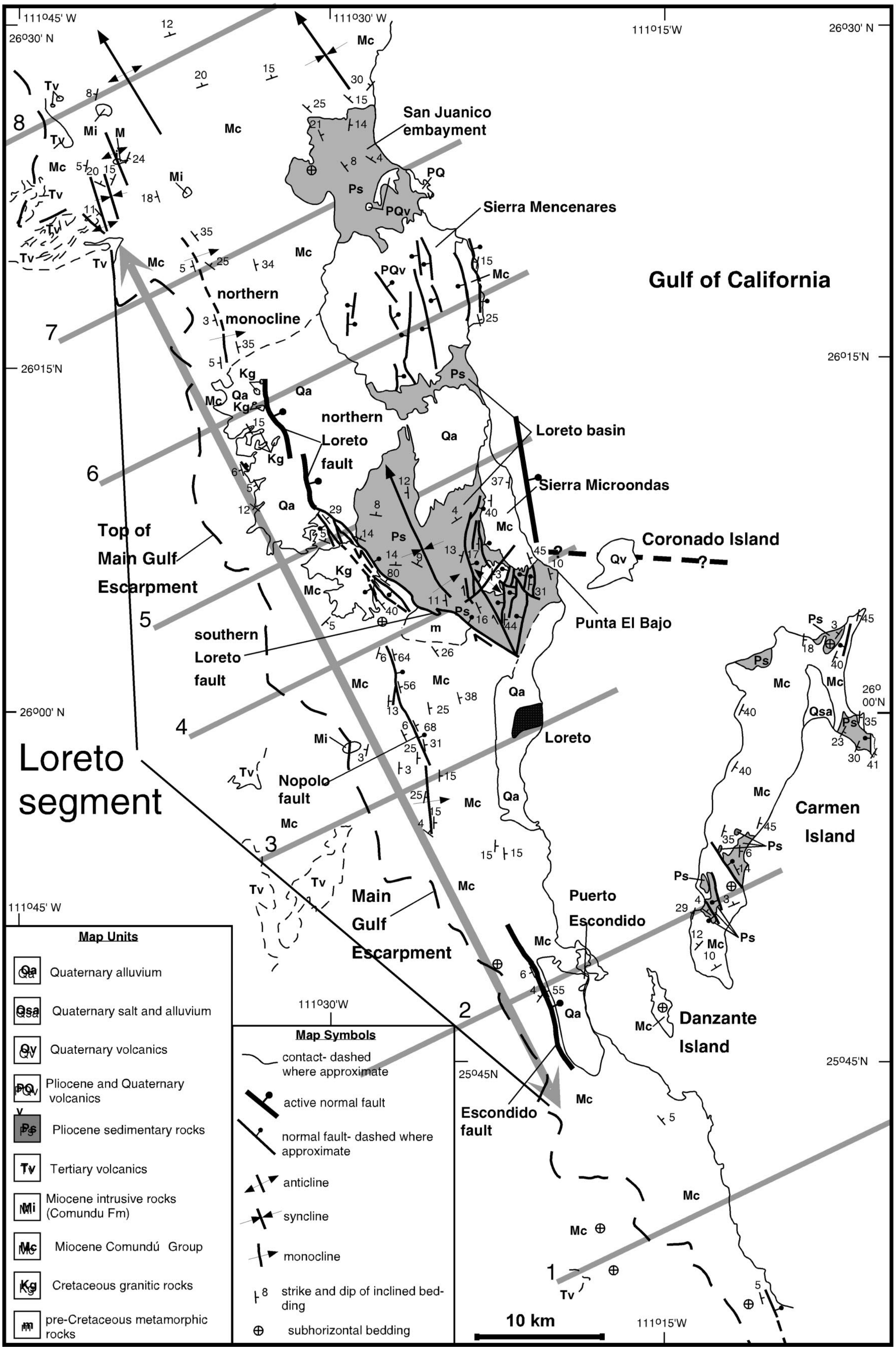

Figure 3. Geologic map of the Loreto region. Gray lines 1–8 show the locations of the profiles in Figures 5 and 6B.

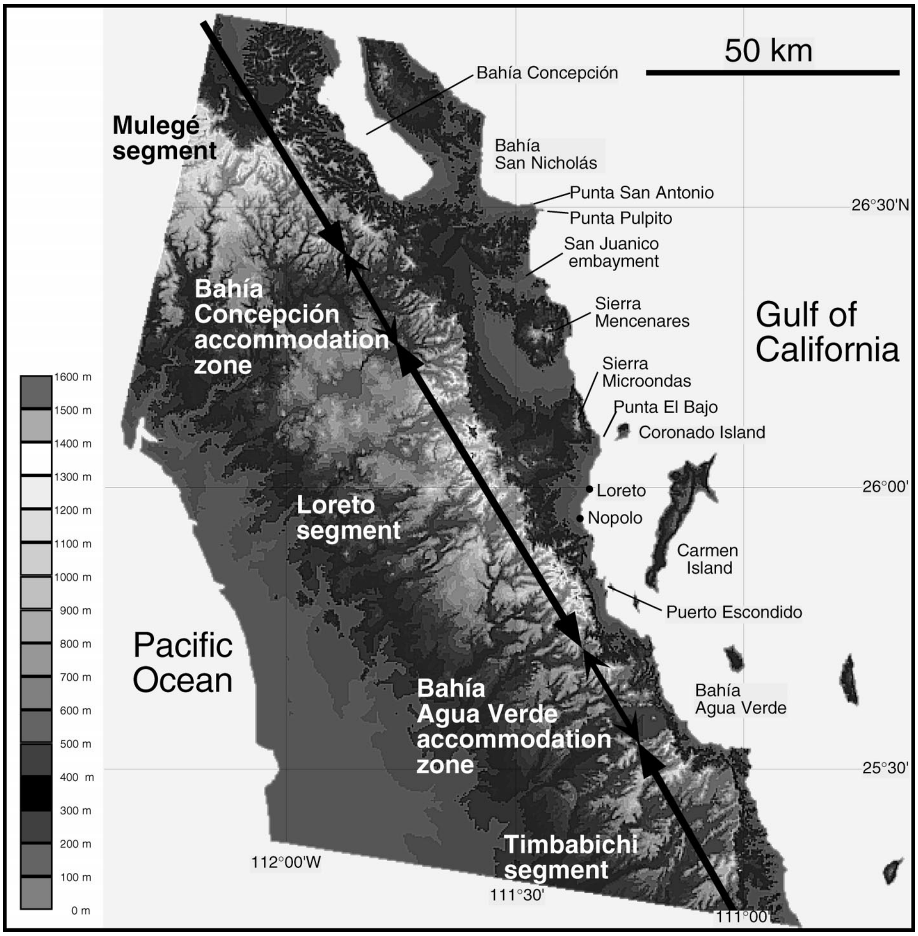

Figure 4. Gray-scale digital elevation model (DEM) of the Loreto region with 100 m contours and many of the geographic locations mentioned in the text. Note the simple west to east division of the peninsula at this latitude into a larger western part with a gentle slope toward the Pacific Ocean and a narrow eastern part with the steep Main Gulf Escarpment facing toward the Gulf of California. The more complex topography on the narrow eastern coastal belt reflects the complex two-stage structural evolution of the plate boundary and the presence of local, young volcanic centers (Sierra Mencenares and Coronado Island). The Main Gulf Escarpment is generally linear along a northwestern trend, but the segmentation is seen in its detailed pattern. Along the Loreto segment, the escarpment is relatively straighter, steeper, and higher than in the accommodation zones to the north and south. The low nature of the escarpment top at the accommodation zones is especially clear on this image. The parts of the Mulegé and Timbabichi segments shown here are stepped to the west and east from the Loreto segment and have a more irregular and a lower escarpment, respectively. Carmen Island has a trend that is distinctly more north-northeast than the other features in the region. See text for further discussion. The DEM is from the North American Landscape Characterization (NALC) triplicate data of Mexico, which contain digital elevation data. These data were provided by Mexico's National Institute for Statistics, Geography, and Informatics (INEGI).

Tectonic Divisions of the Gulf of California and Baja California Peninsula

From north to south, the present topography and geology of the Gulf of California can be divided in two ways. Focusing on the active transform faults in the gulf itself (Goff et al., 1987) and those active faults that diverge from them, the gulf can be divided into three major domains along the rift axis. In the north, from Puertecitos to the Salton trough (Fig. 2A), many strike-slip faults diverge from the transform faults and cut across Baja California and southern California to form the system of transpeninsular faults (e.g., Suarez-Vidal et al., 1991; Humphreys and Weldon, 1991). Thus, the plate boundary is as wide as ~200 km. However, in the central part of the gulf, from lat ~30°N to ~25°N, there are no faults cutting across the peninsula, and few active faults are known along the margins of the gulf (Fig. 2A); most of the faulting appears to be along the transform faults (Goff et al., 1987). Recent data from uplifted marine terraces and shallow seismic surveys in the Loreto region suggest that an important, but unknown, proportion of active faulting is occurring along the Baja California peninsula (Mayer and Vincent, 1999) and in the nearshore shelf (Nava-Sanchez et al., 2001). The Loreto region of this study lies in the southern part of this central domain (Fig. 2B). In the southernmost gulf from ~25°N to the mouth of the gulf, active normal faults—most prominently the seismically active Espiritu Santo fault (formerly termed the northern part of the La Paz fault) (Fig. 2B) (Fletcher and Munguía, 2000)—cut through the western margin and along the Baja California peninsula.

The central Baja California peninsula and shallow offshore shelf and islands can be divided perpendicular to the overall rift axis into a western and eastern region separated by the Main Gulf Escarpment (Figs. 2, 3, and 4) (Gastil et al., 1975). The Main Gulf Escarpment is continuous at a scale of hundreds of kilometers, but varies topographically and structurally, especially at more detailed scales (Figs. 3 and 4). The region west of the Main Gulf Escarpment is a gentle, westward-tilted ramp of mainly nonmarine, volcaniclastic rocks formed in the forearc basin of the Miocene continental volcanic arc and locally overlain by younger basalts (Hausback, 1984; Sawlan and Smith, 1984; Sawlan, 1991). The region east of the escarpment is part of the Gulf extensional province (Fig. 2A), with basin-and-range–style landscape, faults, and local basins and volcanic centers formed during development of the gulf. Axen (1995) showed that the Gulf extensional province in the northern Baja California peninsula, north of Puertecitos (Fig. 2A), is segmented in a fashion similar to that in many other rifts (Fig. 1C) (e.g., East African rift, Bosworth, 1985; Ebinger, 1989a, 1989b). These segments are defined by ~100-km-long normal faults that alternate in dip direction and also the symmetry of the related half grabens.

The current pattern of seismicity in the Gulf of California (e.g., Goff et al., 1987) suggests that the plate boundary in the central and southern gulf has some amount of strain partitioning. Major strike-slip earthquakes are confined to the northwest-striking transform faults in the deep basins of the gulf (Fig. 2B), whereas earthquake motions on the margins mainly show normal slip on north- and northwest-striking faults (Fletcher and Munguía, 2000).

GEOLOGY OF THE LORETO REGION

The coastal belt we studied extends from the southern end of Bahía Concepción to Bahía Agua Verde (~50 km south of Loreto) (Figs. 2B and 3) and from the Main Gulf Escarpment on the west to the coast on the east. We also investigated Carmen Island. The southern 25 km of the coastal belt and much of Carmen Island were studied in a reconnaissance mode. The coastal belt east of the Main Gulf Escarpment consists mainly of a narrow belt of ridges, valleys, and pediments adjacent to the escarpment, low- to moderate-elevation ranges transverse to the coast, and narrow coastal plains (Fig. 4). Breaking this pattern is the circular Sierra Mencenares volcanic complex and the low plain that surrounds most of it. Carmen Island is conspicuously elongate at a moderate angle to the dominant northwest grain of the coastal belt. North of Punta El Bajo, the coastal belt east of the escarpment is 20–30 km wide, and there are only very small islands close to the shoreline (too small to show on these maps) (Fig. 4). South of Punta El Bajo, the coastal belt narrows to only 5 km near Puerto Escondido, and there are numerous large islands (Fig. 4).

Pre–Gulf of California Rocks

Most of the bedrock in the Loreto region consists of volcanic and clastic rocks of the Oligocene to Miocene Comondú Group (Fig. 3) (McLean, 1988; Zanchi, 1994; Umhoefer et al., 2001), which represent a volcanic arc and forearc basin that formed from ca. 30 to 12 Ma (Hausback, 1984; Sawlan and Smith, 1984; McLean, 1988; Zanchi, 1994). The island and coastal exposures of the Comondú Group (up to ~10 km inland) consist of massive andesitic breccia and andesite and basaltic andesite lava flows (McLean, 1988) that form the volcanic-core facies of Hausback (1984). The zone near, and a few kilometers east of, the Main Gulf Escarpment is the proximal facies of Hausback (1984) consisting of massive to bedded volcanic-rich conglomerates interpreted to be lahars interstratified with fluvial conglomerates and sandstones. A few uncommon felsic tuffs are in this facies. A few kilometers west of the Main Gulf Escarpment, the proximal facies changes to the distal facies of the Miocene arc-forearc system, and fluvial sandstones and mudstones dominate with less common conglomerates.

In an ~15-km-wide belt in the footwall of the southern Loreto fault and in isolated exposures in the footwall of the northern Loreto fault (Fig. 3), the Comondú Group rests nonconformably on Cretaceous(?) granitoids and pregranitoid metavolcanic rocks of unknown age (McLean, 1988). Locally in these belts, the Comondú Group rests disconformably on arkosic sandstones that are either (or both) lower Tertiary rocks or basal fluvial strata of the Comondú Group. Exposure of the Cretaceous granite and metamorphic rocks suggests that a Cretaceous arc formed in the region, but the lack of exposure prevents us from delineating any arc segmentation that might affect later rift segmentation.

Syn–Gulf of California Rocks and Structures

From evidence in other parts of the Gulf of California region, it is clear that rift-related extensional faulting began in late Miocene time and that the Gulf of California was a marine seaway by 8–7 Ma (Smith, 1991; Martín-Barajas et al., 1995; Holt et al., 2000). Although there are no known Miocene rocks younger than the Comondú Group east of the escarpment in the Loreto region, we will show that much of the Loreto region shows evidence for late Miocene faulting. In addition, we suggest that some of the erosional retreat of the Main Gulf Escarpment began in Miocene time.

The Loreto basin is a stratigraphically complex transtensional half graben bounded on the west and southwest by the Loreto fault (Fig. 3) (Umhoefer et al., 1994; Zanchi, 1994; Dorsey et al., 1995; Dorsey and Umhoefer, 2000). The lower part of the basin fill is entirely nonmarine. The middle part of the basin fill consists of interfingering fluvial, deltaic, and marine deposits derived from the west and deltaic and marine deposits lying with a buttress unconformity against the Comondú Group in the Sierra Microondas. The upper part of the basin fill is mainly exposed to the north as marine deposits and in the southeast basin as shoreline and nearshore deposits. Marine strata of the Loreto basin are interbedded with numerous tuffs derived from the Sierra Mencenares (Fig. 3), a late Pliocene volcanic complex (Bigioggero et al., 1995). Four of the tuffs give $^{40}Ar/^{39}Ar$ ages of 2.61–1.97 Ma (Umhoefer et al., 1994). The lower nonmarine deposits are undated, but must be mostly Pliocene as they are conformably overlain by the well-dated marine strata with only a transgressive sequence boundary. We estimate that the basin began to form sometime between ca. 6 and 3.5 Ma (Dorsey and Umhoefer, 2000).

The San Juanico embayment, located immediately north of the Sierra Mencenares (Figs. 3 and 4), contains nonmarine and marine strata that interfinger with volcanic rocks of the Sierra Mencenares and are late Pliocene in age. The basin lies unconformably on the Comondú Group. The Sierra Mencenares is a late Pliocene volcanic center that erupted into the northern Loreto basin (Bigioggero et al., 1995; Dorsey and Umhoefer, 2000). The San Juanico embayment made up the northern end of the Loreto basin before the Mencenares volcanic complex isolated the San Juanico from the main basin. North of the San Juanico embayment are two patches of Pliocene strata (Johnson et al., 1997) that formed in separate embayments not connected to the Loreto basin (not shown in Fig. 3). And on Carmen Island there are five patches (kilometer scale) of probable Pliocene strata that are dominated by marine deposits (Fig. 3).

Local Quaternary deposits are common in the region, but extensive Quaternary deposits are found only in the northern Loreto basin, on the west and south sides of the Sierra Mencenares, and in the coastal plains near Loreto and Puerto Escondido (Fig. 3). The northern Loreto basin and Puerto Escondido areas display strong evidence for Quaternary faulting and subsidence. Both areas are bounded on the west by Quaternary faults (Mayer and Vincent, 1999; this study), have flat plains of kilometer scale with little or no incision by arroyos, and sit at a low elevation (Figs. 3 and 4). Quaternary faulting is also known from faults offshore near the coast (Nava-Sanchez et al., 2001), and uplifted marine terraces along the coast of the Sierra Mencenares near Punta El Bajo (Mayer and Vincent, 1999).

RIFT SEGMENTATION OF LORETO REGION

Our work in the Loreto region modifies the position and boundaries of three segments that Axen (1995) proposed (Fig. 2). We provide multiple lines of evidence for the location of the Loreto segment and add much structural and mapping data bearing on the style and temporal interpretation of the segmentation. Our map (Fig. 3) shows the Loreto and Nopolo faults in a similar configuration as that of McLean (1988), but our mapping was at a larger scale and thus has more detail. Our map differs substantially from Zanchi's (1994) map, which does not show a Loreto fault separating the Loreto basin from the older rocks to the southwest. Zanchi (1994) also showed a continuous normal fault along the base of the Main Gulf Escarpment from where we map the northern monocline to the northern end of the Nopolo area, but considerably west of (west of the Cretaceous granite) where we map the Loreto fault. Zanchi (1994) showed no normal fault where we map the Nopolo fault, but we agree on the location of the Escondido fault.

The Loreto segment is 85 km long (northwest-southeast). We locate the northern boundary of the Loreto segment ~25 km south of Bahía Concepción (in the northern part of Fig. 3). There the down-to-the-east structures end, no throughgoing faults extend along the Main Gulf Escarpment north of there, and the escarpment is much lower and less straight for ~20 km than to the south (Figs. 3 and 4). We define the southern boundary of the Loreto segment at the southern end of the Escondido fault, ~5–10 km south of Puerto Escondido (Fig. 3), where again there are no major faults along the escarpment to the south and it becomes lower and less straight (Fig. 4). In this section, we describe the main segments and how the segments are defined. The individual structures will be described in more detail later in conjunction with the structural analysis of the Loreto segment and part of the northern accommodation zone.

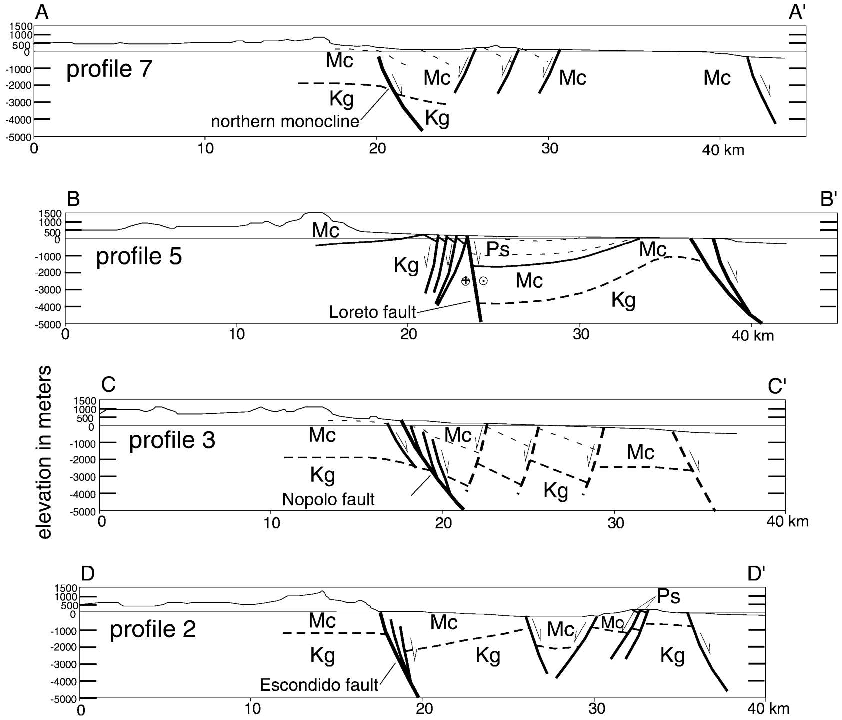

Figure 5. Four serial cross sections through the Loreto segment selected to show the main four structures aligned with the base of the Main Gulf Escarpment. Sections A–A′ to D–D′ correspond to profiles 2, 3, 5, and 7 in Figures 3 and 6, where their locations are shown. Rock units: Kg—Cretaceous granite, Mc—Miocene Comondú Group, Ps—Pliocene sedimentary strata. Thin dashed lines represent bedding. The tilt of individual fault blocks is well defined by surface geology or simple projections, except for the block east of the Escondido fault, which is not well defined and may tilt to the east. The graben offshore in A–A′ (profile 2) is taken from Nava-Sanchez et al. (2001). Note that all of the boundary structures are extensional monoclines or monoclines cut by normal faults. The Loreto fault is the only known major strike-slip fault in the region.

Loreto Segment

The Loreto rift segment is well defined on the basis of topographic, stratigraphic, and structural criteria. However, the segment contains an anomalous part, the Nopolo subsegment, that is interpreted to be an integral part of the segment, but that contains some traits similar to the accommodation zones at the ends of the Loreto segment. The Loreto segment is bounded on the west by a series of four aligned, but discontinuous fault zones with an estimated 1–2 km of offset. These structures are, from south to north, the Escondido fault, the Nopolo fault, the northern Loreto fault, and a monocline north of the Loreto fault (Figs. 3 and 5). All of these structures have down-to-the-east offset, form the westernmost large structure of the segment at that latitude, and lie at or within 2–4 km of the base of the Main Gulf Escarpment. The monocline in the north is a continuation of the en echelon pattern of the northern Loreto fault (Fig. 3). It is significant that major down-to-the-east faults are not found north and south of the Loreto segment for tens of kilometers.

The Escondido fault lies directly at the base of the Main Gulf Escarpment, which is very steep and relatively high behind the fault (Figs. 3 and 6). The Nopolo fault lies within a zone in which the topography rises much more gradually and is crudely stepped. The northern Loreto fault lies 2–4 km east of the base of a steep and high escarpment that rises to nearly 1700 m, the highest point in the Sierra Giganta in the Loreto region.

The topography of the Main Gulf Escarpment west of the Loreto segment increases in elevation from the northern and southern boundaries of the segment toward the central areas behind the major fault zones and forms a broad arch with a conspicuous low area behind the Nopolo fault (Fig. 6). This along-strike elevation gain is ~500–1000 m and mimics the major structures that define the segment (Figs. 5 and 6). The elevation change in the escarpment can be seen in regional topography in a digital elevation model (DEM) of the region (Fig. 3). It is also evident in a series of topographic profiles selected every 10–20 km to show major topographic changes within the region (Fig. 6, A and B) and in a graph of the highest elevations along the escarpment within consecutive 2-km-wide transects along the trend of the escarpment (Fig. 6C).

The steepness and straightness of the escarpment also define the segment. The escarpment is steeper and narrower within the segment, especially west of the Loreto and Escondido faults, and more gentle and wider as the escarpment approaches the segment boundaries. This relationship is depicted in the series of topographic profiles (Fig. 6B). It is also quantified in a steepness index, which was measured as the ratio of the highest relief of the escarpment to the width of the escarpment in a line perpendicular to the escarpment (Fig. 6, C and D). Qualitatively, one can see in the DEM of the Loreto region (Fig. 3) that the Main Gulf Escarpment is much straighter behind the Loreto segment than to the north and south.

The systematically greater relief and steepness indicate segmentation of the flank uplifts that is consistent with structural segmentation. We interpret the rise in elevation and increase in steepness of the escarpment toward the center of the segment to reflect an increase in footwall uplift of the Loreto-Nopolo-Escondido fault system added to any regional, isostatic forces that are uplifting the rift escarpment.

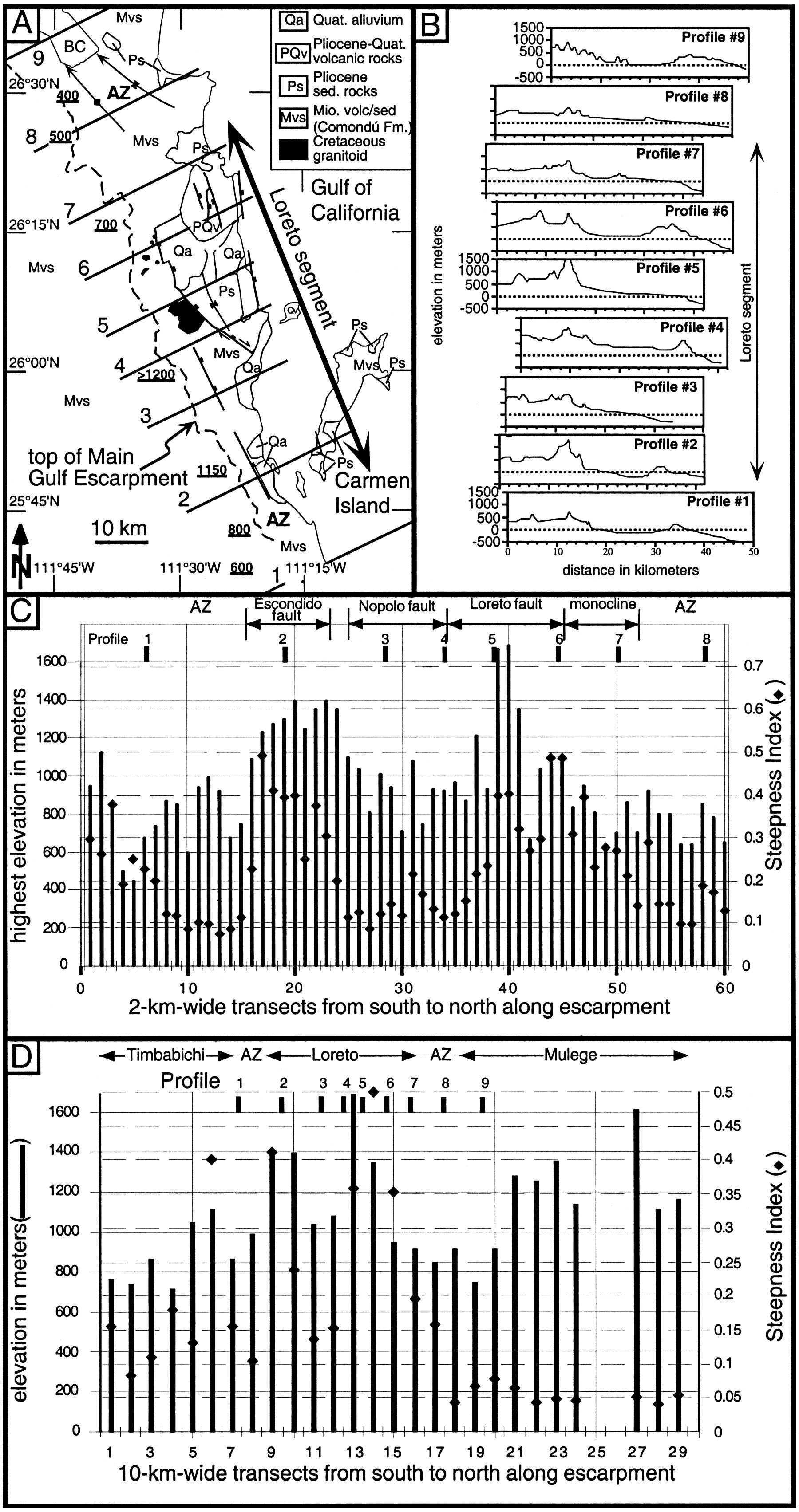

The relationship between topography and segment location is not simple, because there are parts of the segment that have secondary ridges that trend away from the escarpment across the segment (Fig. 3). Topographically, the Nopolo area has a lower and less steep escarpment than the rest of the Loreto segment (Fig. 6, B and C). The Nopolo area also has a coastal plain with an irregular, erosional western edge that is not fault controlled. In contrast, the Nopolo area does include the systematic rise in stratigraphic units discussed next as the final criterion in defining the Loreto segment.

The along-strike elevation of the Main Gulf Escarpment west of the Loreto segment is systematically mirrored by an along-strike arching of stratigraphic units in the footwall of the segment. This arching was documented by tracing the contact between the Comondú Group and unconformably overlying late Mio-

Figure 6. An analysis of the height and steepness of the Main Gulf Escarpment in the Loreto region. (A) Map showing the location of (B) nine topographic profiles. Elevation groupings are shown by arbitrary divisions of the escarpment into (C) 2-km-long and (D) 10-km-long transects perpendicular to the escarpment. The nine lines in A are the locations of the lines of the profiles in B and in Figures 3 and 5. Abbreviations in A: BC—Bahía Concepción, AZ—accommodation zone; the underlined numbers adjacent to the Main Gulf Escarpment (dashed line) give the elevation (in meters) of the base of the late Miocene basalt flows. The profiles in B are aligned on the position of the Main Gulf Escarpment, and their positions along the graphs in C and D are shown. For each arbitrary transect in C and D, the highest elevation of the escarpment is shown by the vertical bar, and the diamond is the steepness factor, which was measured as the ratio of the highest relief of the escarpment to the width of the escarpment in a line perpendicular to the escarpment. The profiles (B) and graphs (C and D) confirm what is qualitatively seen on the digital elevation model (DEM) (Fig. 4) that the escarpment is higher and steeper along the Loreto segment in comparison to the accommodation zones (AZ) to the north and south. The anomalously low and less steep Nopolo area is also clear. The part of the Timbabichi segment (graph D) analyzed here is lower and a little less steep than the Loreto segment, whereas the Mulegé segment is about as high as Loreto but distinctly less steep.

cene basalt flows along the escarpment on 1:50 000-scale topographic maps. We plotted the elevation of this stratigraphic unconformity at seven points where it was confidently identified (bold underlined numbers in Fig. 6A), and it rises ~600–800 m from the borders of the segment to the interior. The Comondú Group along the escarpment is moderately well layered on the 100 m scale as a series of thick sedimentary and volcaniclastic units whose bedding attitudes also show this arching. Because the late Miocene basalts are involved, the arching must have occurred after Miocene time and thus during rifting of the Gulf of California. A second arched stratigraphic datum is the basal contact of the Comondú Group that overlies lower Tertiary arkose or Cretaceous granite and metavolcanic rocks. In the Bahía San Nicholás area (Fig. 3), ~20 km north of the Loreto segment, granite is exposed near sea level (J. Ledesma, 1998, personal commun.). The granite–Comondú Group contact is exposed west of the Loreto fault in many places (Fig. 3), where it is at an elevation of ~300 to ~400 m. South of Loreto, the granite is not exposed in our map area, and it must be below the surface, <100 m elevation (Fig. 5). Localized relief of up to ~100 m on the pre-Comondú surface is restricted to a few inselbergs. These stratigraphic data may reflect the arch of the top of the Comondú Group, or they may indicate a more localized uplift in the footwall of the Loreto fault.

Mulegé Segment

The Mulegé segment (Figs. 2 and 4), north of the Loreto segment, is ~110 km long and has many features that contrast with the Loreto segment (Axen, 1995): no major faults along the base of the Main Gulf Escarpment, mainly west-dipping faults and east-dipping strata, a generally broad Main Gulf Escarpment, and lack of thick synrift basins near the western margin (Wilson, 1948; Wilson and Rocha, 1955; McFall, 1968). Presumably the large fault(s) that controlled the formation of this segment are east of the Gulf of California (Axen, 1995), in contrast to the Loreto segment.

The Santa Rosalía basin is located in the northern part of the Mulegé segment. It contains upper Miocene to Pliocene marine deposits (Holt et al., 2000) that are ~350 m thick and cut by west-dipping normal faults with modest offsets that tilted the strata <15° to the east (Wilson, 1948; Wilson and Rocha, 1955). The largest fault in the southern part of the Mulegé segment is the west-dipping Concepción Bay fault on the eastern side of Bahía Concepción (McFall, 1968). Strata of the Comondú Group dip mainly to the east in the footwall (east) of the Bahía Concepción fault and form an open syncline in the hanging wall of the fault (McFall, 1968). There are only thin, flat-lying sedimentary strata of Pliocene age in the southern part of the Mulegé segment on Punta Chivato (variably a few tens of meters thick) (Johnson et al., 1997) and in the southeast corner of Bahía Concepción (<53 m thick) (Johnson et al., 1997), indicating that deformation was completed by that time in the onshore part of most of the Mulegé segment.

Topographically analyzed 10-km-long strips of the Main Gulf Escarpment in the Mulegé segment indicate elevations that are similar to those in the Loreto segment (Fig. 6D). The Mulegé segment differs substantially from the Loreto segment, however, in that the drainage divide of the peninsula is much farther from the base of the escarpment (20–32 km) than in the Loreto segment (3–8 km) (Fig. 3); thus, the Mulegé segment has a less steep escarpment than Loreto (Fig. 6D).

Bahía Concepción Accommodation Zone

An accommodation zone occupies the 20–25-km-long gap between Bahía Concepción (Fig. 4), which is the southern end of the Mulegé segment, and the Loreto segment. The accommodation zone exposes mainly volcanic and sedimentary rocks of the Comondú Group with a thin embayment of Pliocene(?) strata near Bahía San Nicholás (Fig. 4). Pre–Comondú Group granite of probable Cretaceous age is exposed near Punta San Antonio (J. Ledesma, 1998, personal commun.), and Punta Pulpito is a Quaternary(?) obsidian dome.

The accommodation zone is not well understood structurally. Our 1:50 000-scale mapping of the area suggests that there is little structural relief within the Comondú Group across the zone from west to east. Most of the accommodation zone consists of two open, north-northwest–plunging folds, an anticline and syncline pair (Figs. 3 and 7). An area in the southwestern part of the accommodation zone, near the escarpment, has three north-northwest–plunging folds (kilometer scale) in strata of the Comondú Group (Fig. 3). The middle syncline passes southward into a west-dipping normal fault (too small to show in Fig. 3), suggesting that the folds are all extensional and related to normal faulting. Bedding in places between these folds is gently dipping to the south. Immediately east of these folds is a ridge in which bedding changes from the typical west dips to anomalous south dips (not shown in Fig. 3). Two faults in this ridge form a horst. These relatively complex structures are located north and northwest of the monocline that is the northernmost structural boundary of the Loreto segment, and they may represent the northward decrease in offset of the boundary structure. Likewise, the large syncline in the eastern part of the accommodation zone lies along the southeast projection of the west-dipping Bahía Concepción fault on the Bahía Concepción peninsula and may be related to it (Fig. 7). Thus, it appears that the accommodation at depth consists of overlapping west- and east-dipping normal faults as viewed across the strike of the rift.

Bahía Agua Verde Accommodation Zone and Timbabichi Segment

We were not able to distinguish a boundary between the proposed Bahía Agua Verde accommodation zone and the proposed Timbabichi segment to the south (Figs. 2 and 4). Most of the area south of the Escondido fault has gentle dips of 3°–5°E in massive to thick-bedded volcanic breccias and subordinate lava flows of the Comondú Group. The 15°–20° tilt of local blocks may indicate normal faults that dip to the west. The mesas along and west of the Main Gulf Escarpment are capped by flat-lying lava flows of the late Miocene basalt unit. Numerous dikes cut the Comondú Group where the highway ascends the Main Gulf Escarpment (17 km south of Puerto Escondido). In the northern part of Bahía Agua Verde there is a 4–5-km-long normal fault that dips to the east and has a narrow coastal plain on its hanging wall. The topographic expression of the Main Gulf Escarpment along the Bahía Agua Verde accommodation zone and Timbabichi segment is lower (700–1100 m) and not as steep as in most of the Loreto segment (Fig. 6D). An eastward jump in the escarpment along Bahía Agua Verde and the presence of a normal fault mapped near the coast suggest that faulting may be concentrated along the shoreline, but our study cannot evaluate that possibility.

STRUCTURAL ANALYSIS

The structural framework of the Loreto segment is complex because the main, rift-bounding structure is discontinuous at the surface of the Earth, and the segment that formed in late Miocene time was overprinted by Pliocene to Quaternary transtensional structures. The main rift-bounding structures are the Escondido fault, Nopolo structure, Loreto fault, and monocline north of the Loreto fault (Figs. 3 and 7), all of which strike ~335°. The northern Loreto fault and monocline to the north form an en echelon array stepping to the west and having progressively less offset to the north. Here, these major map-scale faults are described, and then the kinematic analysis of secondary faults is presented.

Escondido Fault

The Escondido fault is a 14-km-long normal fault with down-to-the-east offset (Fig. 3). Its northern half and its southernmost 2 km strike 330°; the south-central part of the fault bends to join these two parts. The fault defines a dramatic escarpment with peaks up to 1400 m high 2 km from the fault (Fig. 3) and very short drainages that make a relatively straight drainage divide (Fig. 4). The Escondido fault is located at the mountain front where it was examined in four locations (Fig. 5A). The fault juxtaposes sedimentary and volcanic rocks of the Comondú Group in its footwall to the west with mainly Quaternary alluvium and local belts of Comondú Group in the hanging wall. The main fault is not well exposed in most locations but is indicated by a change in bedding attitude from nearly subhorizontal or dipping gently west in the footwall to dipping 15°–55°E in the immediately adjacent hanging wall. Near the northern end of the fault, there is evidence of Quaternary displacement along the fault. At one location, a gravel unit is faulted, and in another location there is a degraded fault scarp cutting gravels that sit on a bedrock surface. There are many small faults within ~10 m of the main fault in the footwall, but small faults become widely spaced farther than ~10 m away from the main fault.

The hanging-wall belts of Comondú Group rocks consist of two areas of foothills that are part of the fault zone and two transverse ridges to the north. The foothills are 1–2 km long and 100–500 m wide and contain sandstone, conglomerate, and bedded volcanic breccia. The foothills have small faults at a spacing of 1–2 m that are mainly southwest dipping with subordinate northeast-dipping faults. Bedding dips 30°–55°E in the foothills block. In the hanging wall of the northern part of the Escondido fault are two ridges, >300 m high, with ridgelines oriented transverse to the fault. These ridges consist of lava flows and massive volcanic breccia, in contrast to the dominantly sedimentary rocks that compose the foothills belts immediately adjacent to the mountain front. These transverse ridges have crude subhorizontal to gently east-tilted layering.

Nopolo Fault and Monocline

A major structure west of Loreto and Nopolo is aligned with the Escondido fault across

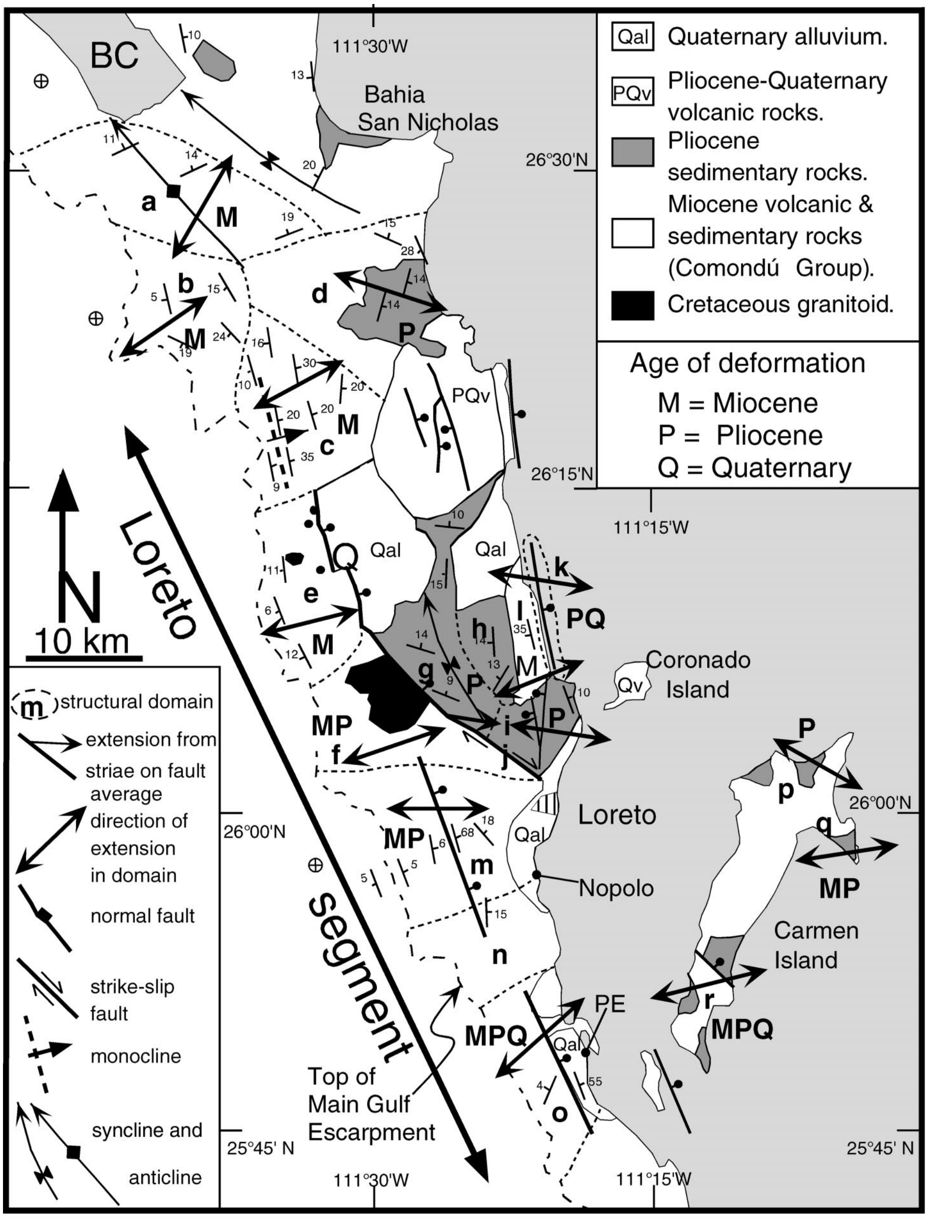

Figure 7. Simplified structural map of the Loreto region showing simplified geology, structural domains (labeled with letters and short-dashed boundaries), average extension direction in each domain (shown by large arrows), and inferred age of deformation of each domain (shown by large letters). The age of deformation is based on (1) the age of the rocks that the faults cut and (2) the consistent pattern of domains with only Miocene Comondú Group rocks having a northeast-southwest (to east-northeast–west-southwest) extension direction, whereas domains with Pliocene rocks have an east-west (to west-northwest–east-southeast) extension direction. Abbreviations: BC—Bahía Concepción, PE—Puerto Escondido.

an ~10-km-long gap. This structure and the area around it with an anomalous escarpment defines the Nopolo subsegment, which is entirely underlain by volcanic and volcaniclastic rocks of the Comondú Group and has a thin cover of Quaternary alluvium in a 3-km-wide coastal plain (Fig. 3). The Nopolo fault is analyzed in more detail by Willsey et al. (2002). The structure at the boundary of the rift segment in the Nopolo subsegment is a down-to-the-east extensional monocline that has been offset by steep normal faults only by 20–30 m (see Willsey et al., 2002, for more details). The extensional monocline faces to the east along the northern 10 km (Fig. 5B) and becomes a broad monocline for 5 km to the south (Fig. 3). The Nopolo extensional monocline is a zone of moderately to steeply east-dipping sedimentary strata 200–400 m wide that has numerous small to moderate normal faults subparallel to bedding. Large faults may be present but are not readily identified. The zone of relatively steep, faulted strata grades to the west into a 200–500-m-wide zone of strata dipping 15°–30°E with small faults spaced at a meter scale. More than 1 km west of the Nopolo fault is a 4–6-km-wide zone with 3°–6°E-dipping strata on the east side and horizontal to 3°W-dipping strata at the top of the escarpment on the west side. This western zone has only widely spaced normal faults. Near the Nopolo fault there is a change in the Comondú Group from well-bedded sandstones to dominantly massive volcanic breccia and minor lava flows. Bedding from here to the coastal plain mainly dips 15°–35°E. Although we expected to observe west-dipping faults in this area on the basis of these bedding orientations, such faults are difficult to find.

Loreto Fault

The Loreto fault and the footwall fault zone lie 4–6 km north of the Nopolo fault. The Loreto fault has two main parts. The southern part juxtaposes Pliocene strata of the Loreto basin on the northeast against (from south to north) lava flows of the Comondú Group; metavolcanic rocks, sandstones, and volcanic breccias of the Comondú Group; Cretaceous granite; and sandstones and tuffs of the Comondú Group (Fig. 5C) (McLean, 1988). The topography rises gradually across the southern Loreto fault, but there is neither abrupt rise at the fault nor any fault scarp. This part of the fault is clearly inactive. The southern part of the fault strikes 310°–315°, dips 70°–80°NE and has consistent fault lineations that indicate dextral-normal slip (Fig. 8) (Dorsey and Umhoefer, 2000).

In contrast to the southern Loreto fault, the northern part of the fault juxtaposes two very different morphostratigraphic units. The hanging wall is a low, little-dissected alluvial plain with no outcrop of bedrock. The footwall is an erosional pediment cut by arroyos with inset straths mantled with Quaternary alluvium (Mayer and Vincent, 1999). Isolated hills of Comondú Group, Cretaceous granite, and older metavolcanic rocks are found west of the fault and east of the Main Gulf Escarpment (Fig. 3). A multiple-event fault scarp runs the entire length of both fault strands of the northern Loreto fault (Mayer and Vincent, 1999). The fault scarp is ~4–7 m high, and the pediment in the footwall rises as much as 35 m above the alluvial plain to the east. The northern part of the Loreto fault has two en echelon faults. The southern fault segment strikes ~350° and then steps 1 km to the west to a northern fault segment that has two 350°-striking parts connected by a northwest-striking bend (Fig. 3).

The footwall of the southern Loreto fault north of the Nopolo fault is a series of moderate-elevation hills that contain a fault zone 2 km wide (Fig. 3). The footwall fault zone has 3–5 west- to southwest-dipping normal faults that are parallel, but antithetic, to the Loreto fault. In three locations these faults bend to the northwest and merge with the Loreto fault. Bedding in the Comondú Group in most of the footwall fault zone dips 25°–40°NE. Within ~200 m of the Loreto fault, bedding steepens to 60°–80°NE. Strata in the Comondú Group west of the footwall fault zone and north of the Nopolo fault dip 5° or less. The footwall of the northern Loreto fault contains isolated exposures of mainly granitic and metavolcanic rocks within 2 km of the fault. Two patches of sandstone of the Comondú Group in the footwall of the northern fault dip 12°–18°E. In numerous arroyos 2–5 km west of the northern Loreto fault, fluvial sandstone and conglomerate and minor eolian sandstone of the Comondú Group overlie a thin section of arkose and grus that in turn overlie granitic rocks. Bedding in this zone dips 10°–26° mainly to the west, and small normal faults are common at meter-scale spacing. Three ~1-km-long faults with at least tens of meters of normal separation lie at or within ~500 m east of the base of the rift escarpment, but there is no throughgoing large fault along the escarpment. One fault is west dipping and two are east dipping. In two areas the strata dip radially away from paleohighs of granitic or metavolcanic rocks and indicate significant primary dip. Near the base of the escarpment, the dip of the strata decreases to 6° or less to the west, and the fluvial sandstone and conglomerate facies is overlain by a thin eolian sandstone and then by an ~50–60-m-thick sequence of tuffs and tuff breccias of the Comondú Group that make up the lower part of the escarpment.

Northern Monocline

The next large structure north of the Loreto fault is a monocline at the base of the escarpment (Figs. 3 and 5D) The monocline is stepped 3 km west from the northern edge of the Loreto fault, continuing the west-stepping pattern of the northern Loreto fault (Fig. 3). The monocline runs 9–10 km north-northwest along the escarpment in lava flows and tuffaceous breccias of the Comondú Group that are the continuation of the tuffaceous unit to the south. This flow and tuffaceous breccia unit is folded in the monocline with dips of 25°–40°E so that the basal sandstones and conglomerates are not exposed. To the east of the monocline, there is a large pediment with thin alluvium covering breccias and flows of the Comondú Group that are exposed in scattered inselbergs. The flows in the inselbergs consistently dip 25°–42°E to northeast, suggesting that there are west- to southwest-dipping faults cutting the Comondú in this area. East of the pediment are some high hills of Comondú Group rocks that are mainly flows and breccias and the Pliocene Mencenares volcanic complex.

Domain Analysis

The analysis of bedding orientation and faults with striae in structural domains in the Loreto region indicates a consistent pattern of two stages of faulting. Domains were defined on the basis of the location of major faults and the age of the bedrock (Fig. 7). The onshore domains can be divided most simply into two types. One type of domain has faults that cut Pliocene strata and thus are late Pliocene to Quaternary in age. Other domains have only lower to middle Miocene rocks of the Comondú Group and thus permissibly can be late Miocene to Quaternary in age. With a couple of exceptions, a clear pattern of the style and kinematics of faulting emerges from these two sets of domains (Fig. 9). Our interpretations essentially agree with, and extend, the results of Zanchi (1994) on the kinematic history of the Loreto region.

The bulk extension in each domain was determined by using the kinematic analysis method of Marrett and Allmendinger (1990). This method determines a direction of maximum shortening and extension for each fault in which the attitude and fault lineations (striae) were measured. All faults measured here were secondary faults with small amounts of offset (millimeters to a few tens of meters) or secondary faults in a larger fault zone. In a domain, each fault is treated as if it contributed an incremental strain to the bulk strain. Thus, this method is similar to the seismologic approach for the derivation of compression (P) and tension (T) axes in a fault-plane solution for an earthquake. Here, each domain is treated as a coherent area that contains a related set of faults, so that we report one combined T-axis and one combined P-axis for each domain. The T-axis for each domain equates to the direction of bulk extension if the T- and P-axes are subhorizontal and subvertical, respectively.

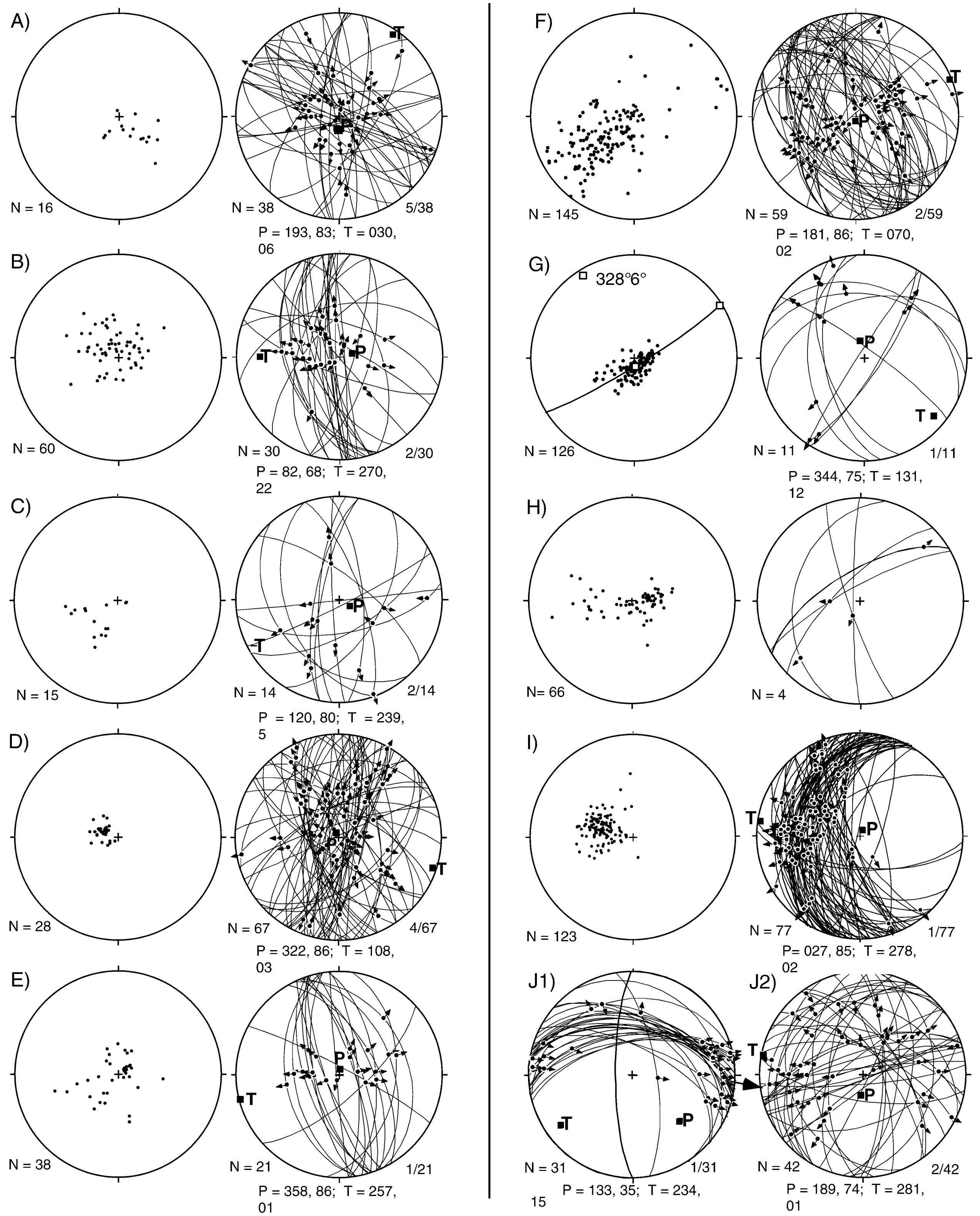

Figure 8. Lower-hemisphere, equal-area stereonets of poles to bedding in left columns and faults with striae in right columns (except domains J and K where faults with striae are in both columns). The domains A to R are shown in Figure 7. Faults with striae are depicted as the great circle of the fault plane, and the dot with the arrow is the lineation of the striae and the direction of motion of the hanging wall of the fault. P and T are the compression and tension axes, respectively, combined from the results of a strain analysis of each domain after the method of Marrett and Allmendinger (1990). The trend and plunge of the P-axis (*Continued on facing page*)

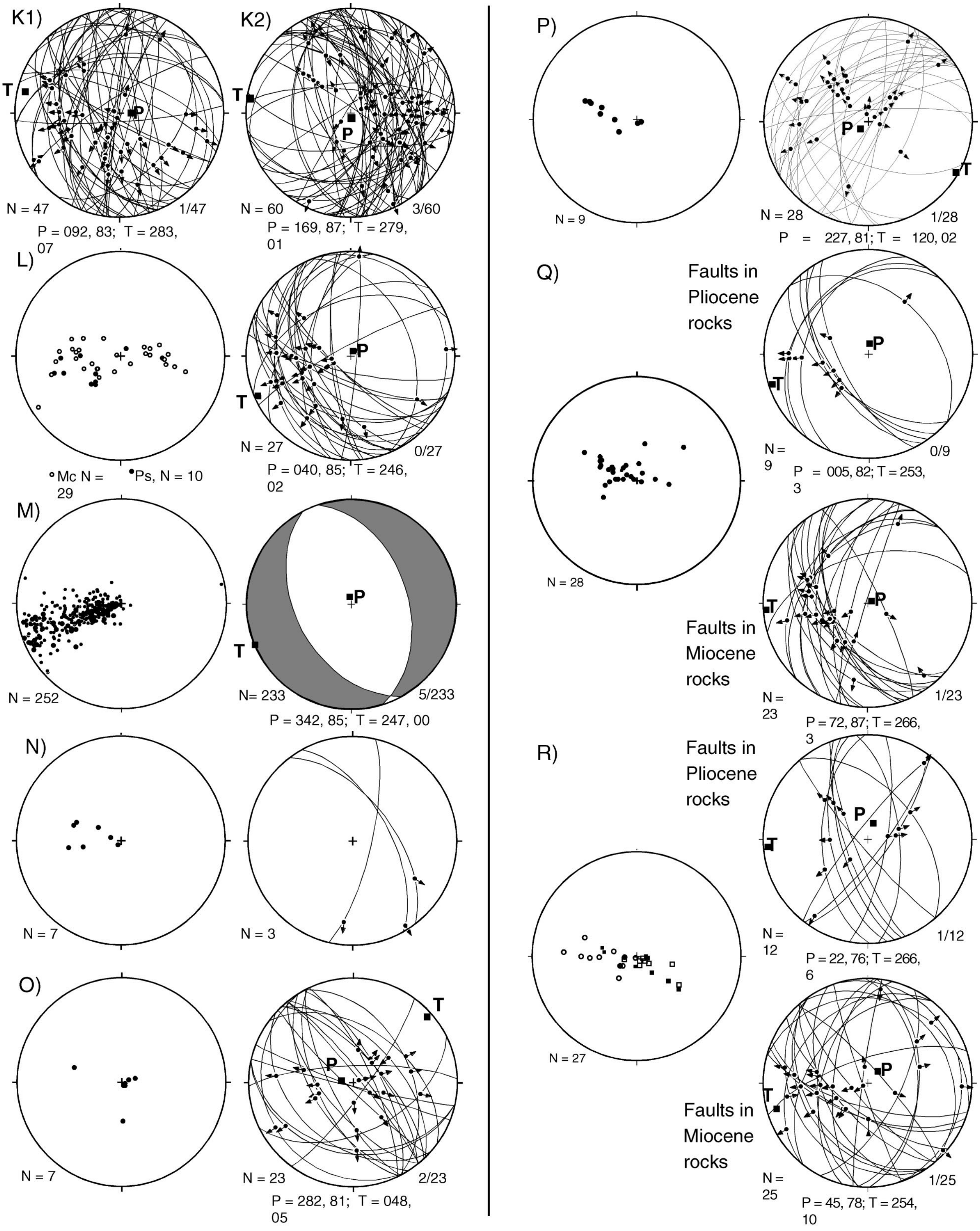

Figure 8. (*Continued*) and T-axis are listed below each stereonet. The ratios on the lower right side of the stereonets in the right columns are the number of faults that fall outside the determined P-axis and T-axis results by >10° over the total number of faults in that domain. In stereonet L, Mc is Miocene Comond Group, and Ps is Pliocene sedimentary rocks.

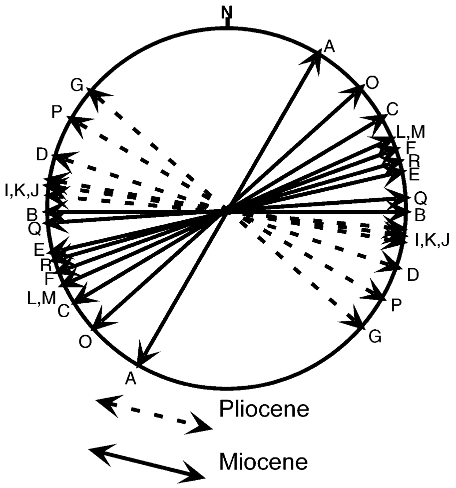

Figure 9. Azimuths of extension for the domains (see Fig. 7) of the Loreto segment and the Bahía Concepción accommodation zone. The domains are labeled on the outside of the circle. The extension directions from domains with definite Pliocene to Quaternary faulting based on the presence of known Pliocene strata are shown dashed; all others are solid. Note how the extension direction in Pliocene to Quaternary domains is consistently more westerly to northwesterly than in the Miocene domains and indicates a change of extension direction from Miocene to Pliocene time of ~30°–35°. See text for discussion.

The assumptions of this method cannot be rigorously tested in a regional study such as this. In Figure 8, however, we do report in the lower right of each stereonet how many individual faults in each domain have P- and T-axes that fall >10° outside the combined P-axis and combined T-axis for the domain. This number in conjunction with the total number of faults in the domain indicates the proportion of faults in the domain that are inconsistent with the extension direction given by the T-axis. Note that few faults in any domain are inconsistent with the strain analysis, which suggests that the faults in a given domain mainly formed in the same stage of faulting. Because we have good evidence for two stages of faulting in the region (Zanchi, 1994; this study), it is likely that some minor part of the faults in each domain were not formed in the same stage as the others. Domain A has a higher number of anomalous faults (13%), and it may have mixtures of faults from two events as discussed subsequently.

Pliocene to Quaternary faulting can be demonstrated in domain D in the San Juanico embayment, in domains G, H, and I in the Loreto basin, and in domain J along the Loreto fault (Fig. 7) because faults in these domains cut dated Pliocene strata. In all these domains, bedding is gently to moderately inclined to the east or distributed along an open syncline in the Loreto basin (domains G and H, Fig. 3). Faults in these domains are moderately to steeply dipping and vary from northwest to northeast striking. The faults are mixed populations of normal and dextral-oblique faults with a minor group of sinistral-oblique faults (Fig. 8). The bulk extension direction in these domains is consistently west-northwest–east-southeast to northwest-southeast, varying from 278°–98° to 311°–131° (Fig. 8). The Loreto fault, which clearly slipped during formation of the Pliocene Loreto basin (Dorsey and Umhoefer, 2000), has fault striae in clay gouge that show dominantly dextral slip with the hanging wall moving toward 94° (Fig. 8, domain J1), consistent with the kinematics of normal faults in other domains of Pliocene to Quaternary age. However, note that the bulk extension direction from this set of striae (Fig. 8A, domain J1) is not horizontal and is not parallel to the extension direction from the other domains with Pliocene rocks.

Faults that cut only lower to middle Miocene rocks of the Comondú Group are in domains A, B, C, E, F, L, M, N, and O. Bedding in these domains varies from gentle to steep and mainly dips to the east to northeast (Fig. 8). Bedding orientations are much more variable in domains A and B of the Bahía Concepción accommodation zone (Fig. 8). The fault populations in these domains are consistently dominated by northwest- to north-striking normal faults, and only a few significantly oblique-slip faults (Fig. 8). These domains also consistently show a northeast-southwest direction of bulk extension.

The dominant normal faults and extension direction in the domains with rocks of the Comondú Group are a major contrast to the domains with demonstrably late Pliocene to Quaternary faulting (Fig. 9). This disparity suggests that the faulting in the domains with Comondú Group rocks is dominantly pre-Pliocene or of middle to late Miocene age (12 to ca. 5 Ma). The faulting pattern also suggests that there was a significant change in faulting from the late Miocene to the Pliocene. In summary, the inferred late Miocene faulting was virtually all normal faulting with an extension direction of east-northeast–west-southwest. By the late Pliocene, faulting shifted to a mixed-mode of normal and dextral strike-slip faulting; dextral-normal (oblique) faulting was common, and the extension direction rotated to west-northwest–east-southeast.

Domain B is somewhat different from the other domains having rocks of the Comondú Group in that the extension direction there is east-west instead of northeast-southwest. This is probably because this domain contains a mix of faults that formed in Miocene time and later or because there were too few faults measured. Domain B has local evidence for mixed old and young faulting. Twenty-one of the 30 faults in domain B are from a fault zone with 15 m of offset on the main fault and numerous secondary faults with decimeter- to centimeter-scale offset between that fault and a larger one. The secondary faults have striae with clear overprinting relationships so that old and young faults could be differentiated (Fig. 10). Note that the older fault set contains both normal and sinistral-normal faults with a east-northeast–west-southwest extension direction, whereas the younger faults are normal to dextral-normal faults with a west-northwest–east-southeast extension direction. This result confirms earlier studies in the Loreto to Santa Rosalía region (Angelier et al., 1981; Zanchi, 1994; Umhoefer and Stone, 1996).

The structural data from Carmen Island can be divided into two groups. Domain P along the northern part of the island contains virtually all faults that cut the Miocene Comondú Group where there are no Pliocene strata. The faults are dominantly northeast-striking, northwest-dipping normal faults and show northwest-southeast extension similar to that in the domains where faults cut Pliocene strata onshore (Fig. 8). The second group of faults on Carmen Island are from domains Q and R on the northeastern and southern parts of the island. These faults are mainly mixed normal and dextral-normal with a minor population of sinistral-normal faults. The extension direction is east-west to east-northeast–west-southwest and does not systematically vary with the age of the rocks. We thus suggest that Carmen Island rotated clockwise; therefore, the meaning of these structural orientations is uncertain until that hypothesis is tested.

Rotation of Carmen Island

The trend of Carmen Island and the orientation of bedding suggest that the island rotated clockwise ~35°–40°. Many islands in the Gulf of California are elongate (Fig. 2B). Most islands trend northwest, parallel to the rift and the Quaternary normal faults (Goff et al., 1987), or north, perpendicular to Pliocene and Quaternary normal faults (Angelier et al., 1981; Zanchi, 1994; Umhoefer and Stone, 1996). Carmen Island is the only island in the gulf that trends north-northeast.

Bedding in Miocene rocks is consistent over large areas along the coast and on Car-

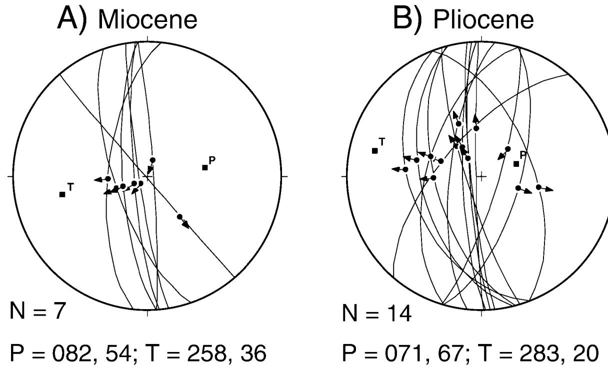

Figure 10. Structural analysis of a population of faults from domain B (Fig. 7) following the methods of Marrett and Allmendinger (1990). The combined P-axis and combined T-axis for each set of faults are given as the trend and plunge of the axis. This population includes secondary faults from one fault zone where overprinting relationships of fault striae are evident such that the striae can be divided into (A) older and (B) younger sets. The rocks being faulted are lower to middle Miocene rocks of the Comondú Group, so faulting could be any age younger than middle Miocene. The Miocene and Pliocene designations are interpretations based on the arguments in the text and in Figures 7 and 9 for the age of faulting. Note that the extension direction (trend of T-axis) changes 25° to the northwest from the older to the younger faults, similar to the pattern found in the whole Loreto region.

men Island because these domains are dominated by simple normal faults. Thus, bedding in the Miocene rocks was used to check for possible rotation of Carmen Island. The Pliocene rocks were not included in this analysis because the Pliocene strata of the Loreto basin have large folds and strike-slip faults that have resulted in complex patterns in the strike of bedding. Bedding on Carmen Island strikes approximately parallel to the trend of the island. The mean bedding for the Miocene rocks in domains P, Q, and R (Fig. 8) strikes 008° and dips 18°E (Fig. 11). The mean bedding onshore in the Miocene was taken from domains C, E, F, L, M, N, and O (Fig. 8) because they are entirely Miocene and lie within the Loreto segment. That bedding strikes 328° and dips 25° to the northeast (Fig. 11). The average strike of the four main rift-bounding structures is 335°. We assume that most of the tilting of bedding in the Comondú Group occurred in the late Miocene as we have previously discussed in this paper. On the basis of the comparison of the mean bedding in the Comondú Group on Carmen Island to the mean bedding onshore, we suggest the island has rotated 40° since the late Miocene (Fig. 11). If we compare the bedding on Carmen Island to the average strike of the rift-bounding structures, then a clockwise rotation of 33° is suggested (Fig. 10). Clearly, paleomagnetic data are required to test whether Carmen Island has rotated as the trend of the island and bedding orientations suggest.

DISCUSSION

History of Loreto Segment

There is no evidence for regional extensional faulting during formation of the Comondú Group in early to middle Miocene time (Zanchi, 1994; Umhoefer et al., 2001). On the basis of the evidence for timing of faulting given here, we conclude that widespread normal faulting occurred during the protogulf stage (12 to ca. 6 Ma) in the Loreto region. This episode of faulting included little to no strike-slip faulting in the Loreto segment and had an east-northeast–west-southwest regional bulk extension direction. Averaging the extension direction of the six domains (domains C, E, F, L, M, and O) in the Loreto segment where faults were measured entirely in the prerifting Comondú Group gives an extension direction of 244°–64°. This result is nearly perpendicular to the 335° overall strike of the main down-to-the-east structures that bound the Loreto segment (Fig. 12). These results strongly suggest that the rift-bounding structures and the secondary faults in the Miocene Comondú Group were initially formed together in late Miocene time. These results also suggest that the younger transtensional stage of deformation was concentrated in only parts of the segment, and much of the segment with only Comondú bedrock became largely inactive.

The discontinuous, and yet aligned, nature of the rift-bounding system of structures (Fig. 3) suggests (1) that they were emanating from a continuous middle-crustal fault zone on which relatively moderate offset had occurred in late Miocene time, and (2) that some parts of the system died after the protogulf stage. These structures—in particular, the common panels of east-dipping rocks in the hanging wall immediately adjacent to the normal faults—all have evidence that they formed initially as extensional monoclines or forced monoclines above major normal faults. The monoclines were subsequently broken by the normal faults as the faults grew and splayed upward toward the surface. The four rift-bounding structures show all stages in this structural evolution (Fig. 5). On the basis of the Nopolo fault, which we explain in the next section is inactive and was formed mainly in the late Miocene, we estimate that the late Miocene offset on the rift-bounding structures was ~500–1000 m.

The existence of a broad erosional surface cut on the Comondú Group rocks and pre–Comondú Group rocks west of the northern Loreto fault suggests a significant period of

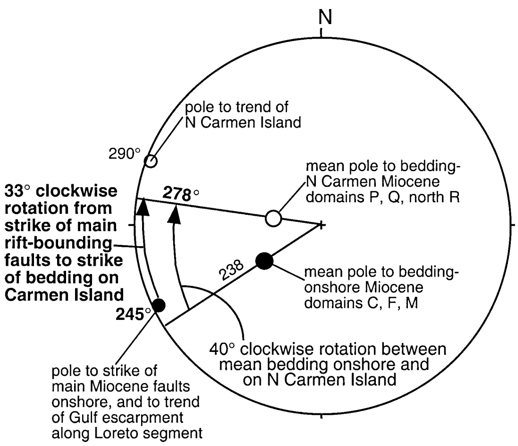

Figure 11. Lower-hemisphere stereonet showing the data that support the clockwise rotation of Carmen Island ~30°–40°. Data from Carmen Island are in white circles, and data from onshore Loreto region are in black circles. Bold lettering gives our preferred interpretation. See text for discussion.

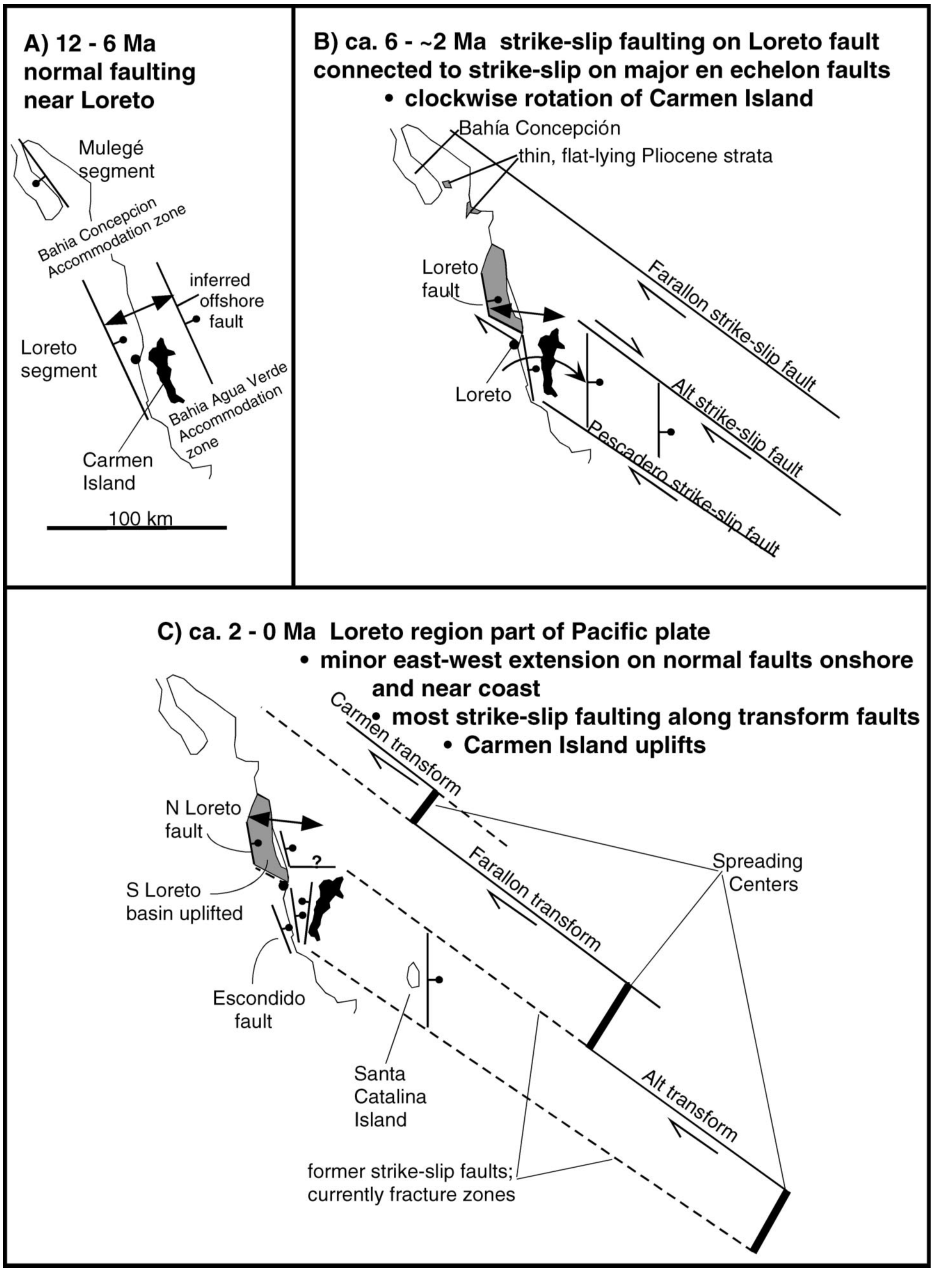

Figure 12. Our model for the evolution of the Loreto region. The present shoreline from Bahía Concepción to Bahía Agua Verde (Fig. 4) is shown in each stage. The large two-sided arrows are the average extension direction for each time interval from this study. Solid lines are faults interpreted to be active at that stage, and dashed lines are inactive faults. Only large features are shown here. The timing of the change from stages A to B is approximate and is from data from the Loreto region (Dorsey and Umhoefer, 2000; this study) combined with data from the whole Gulf of California, in particular the summary of Lonsdale (1989). Data from the Loreto region restrict the time of the transition from B to C to ca. 2.3–2.0 Ma. The offshore transform faults and fracture zones are from Figure 2B and the references cited therein. The graben west of Carmen Island in C is from Nava-Sanchez et al. (2001). Offshore normal faults are conjectural on the basis of steep bathymetric lineaments (Fig. 2).

tectonic quiescence or a slowing of faulting following the creation of the fault-generated topographic escarpment. The formation of the broad erosional surface west of the Loreto fault may extend back into the Miocene. Extensive basalt flows were erupting west of the extensional faults on the Baja California peninsula (Sawlan, 1991), but no volcanism is known from the Loreto segment during protogulf time (cf. Zanchi, 1994, and Umhoefer et al., 2001). The Mulegé segment to the north also contains evidence for extension during the protogulf stage as sedimentary and volcanic rocks near Santa Rosalía have been dated as late Miocene (Holt et al., 2000). In addition, movement on the major fault east of Bahía Concepción occurred in the late Miocene because the fault is overlain on its southern end by flat-lying Pliocene strata (McFall, 1968; Johnson et al., 1997).

The widespread normal faulting of protogulf age was overprinted in Pliocene time by a distinctly different style of transtensional faulting (Zanchi, 1994; Umhoefer and Stone, 1996). The dominant fault in this stage, the Loreto fault, caused subsidence of the >1-km-thick Loreto basin in Pliocene time (Figs. 3, 4, and 12) (Dorsey and Umhoefer, 2000). The northern Loreto fault was likely a normal fault since the late Miocene, whereas the southern Loreto fault cut across older structures as a dextral-normal fault. All domains in the Loreto segment with faulting confined to definitively Pliocene rocks—and therefore of latest Pliocene to Quaternary age—have mixed normal, oblique, and dextral strike-slip faults and a west-northwest–east-southeast extension direction. Domains D, G, H, I, and J2 have a combined extension direction of 281°–101°, which is rotated clockwise ~35° from that in the protogulf stage. Striae within clay gouge of the Loreto fault have an average azimuth of 94°, similar to the Pliocene–Quaternary extension direction from secondary faults. Unlike the relatively thick Pliocene strata of the Loreto basin, patches of only thin Pliocene strata are found in the adjacent accommodation zones. A major volcanic complex in the Sierra Mencenares erupted into the northern Loreto basin near the Bahía Concepción accommodation zone in latest Pliocene time (Fig. 7). This transtensional overprinting is similar to that reported by Angelier et al. (1981) for the larger region from Loreto to Santa Rosalía and agrees with the results of Zanchi (1994) for the Loreto region.

From ca. 6 to 2.0 Ma, the Loreto fault may have linked to a system of faults offshore that included northwest-striking dextral faults and north- to north-northwest–striking normal faults (Fig. 12). We suggest that two of these dextral strike-slip faults were the early Alt and Pescadero faults that evolved to become the Alt and Pescadero transform faults (Figs. 2 and 12) (Ness and Lyle, 1991). The 6–2 Ma interval is when Carmen Island may have rotated 35°–40° clockwise; as a block, it was caught between these major strike-slip faults and between normal faults on its east and west sides (Fig. 12B).

Many lines of evidence support the hypothesis that the Loreto fault was connected to the offshore faults. (1) The southern Loreto fault had a short period of rapid strike-slip faulting at ca. 2.4 Ma that represents a major part of the rate of motion of the plate boundary (~50%). The southern Loreto fault has fault lineations on clay gouge with a rake that averages ~15° on a 70°–80° dipping fault. The Loreto basin, which formed from faulting on the Loreto fault, had a short period of vertical subsidence of 8 mm/yr based on stratigraphic analysis (Dorsey and Umhoefer, 2000). The geometry of the fault and fault lineations and the vertical subsidence rate imply a rate of strike-slip faulting of ~20–30 mm/yr. (2) The period of rapid faulting of the Loreto fault (at ca. 2.4 Ma) is well dated and was nearly synchronous with the initiation of transform faulting (at ca. 2.5 Ma from Lonsdale's [1989] analysis). (3) All field evidence suggests that the Loreto fault does not extend southeast of where it is mapped ~5 km north of Loreto. It does not show up on shallow seismic lines offshore east of Loreto (Nava-Sanchez et al., 2001). In fact, these echo-sounder lines show north-striking normal faults east of Loreto. It appears that the Loreto fault linked to normal faults east of Loreto as well as, we speculate, to a complex east-trending fault zone north of Carmen Island that accommodated the rotation of the island. The presence of the Quaternary volcano composing Coronado Island (Bigioggero et al., 1988) within the proposed east-trending fault zone supports this interpretation. (4) Deformation along the north shore of Carmen Island supports clockwise rotation. Striated faults in domain P form a consistent family of north- to northeast-striking, northwest-dipping normal and dextral-normal faults with a bulk extension direction of 300°–120° (Fig. 8). Note that if the domain is restored 20° counterclockwise, the extension direction is the same as that in the Loreto basin (Fig. 8, domain L). This amount is only part of the 30° of clockwise rotation we propose for Carmen Island in the Pliocene to Quaternary. (5) The southern Loreto fault and Alt and Pescadero fracture zones are collinear within a few degrees and subparallel to plate motion.

The proposed Loreto-Alt-Pescadero fault system is similar in its style and pattern of faulting to the greater Death Valley system (Serpa and Pavlis, 1996). The Loreto system of faults also shows evidence for rapid, dynamic shifts in the locus of faulting as has been documented for Death Valley. For example, after moving at ~50% plate-boundary rates for a short time at ca. 2.4 Ma, the southern part of the Loreto fault died between 2.3 and 2.0 Ma, when faulting largely shifted to a coastal system. This coastal fault system had a much slower rate of faulting than the older Loreto fault (Fig. 12). Likewise, the southeast Loreto fault array was part of this coastal system in latest Pliocene time, but died by late Quaternary time (Dorsey and Umhoefer, 2000).

The fault pattern in the late Quaternary is partly a continuation of that in the Pliocene in which deformation by faulting mainly moved to the east into the offshore region. Normal faulting, however, was dominant, instead of mixed strike-slip and normal faulting. The Escondido and northern Loreto faults, parts of the rift-bounding system, had late Quaternary activity, but at low rates (Figs. 3 and 12) (Mayer and Vincent, 1999). Both faults have subhorizontal, undissected Quaternary alluvial plains in their hanging walls. The northern Loreto fault has a distinct fault scarp, whereas the Escondido fault has a zone a few hundred meters wide of uplifted Quaternary gravels with marine shells indicating >100 m of uplift of the central part of the fault zone. The northern Loreto fault has evidence for 30 m of Quaternary slip and 5 m of slip since the latest Pleistocene (Mayer and Vincent, 1999), i.e., a slip rate of ~0.2 mm/yr, one-and-a-half orders of magnitude lower than that of the Pliocene Loreto fault. The southern end of the Sierra Microondas fault, which continued into the southeast Loreto fault array in the latest Pliocene, now probably forms a major bend to the east (Fig. 12). In order to explain late Quaternary uplift of marine terraces at Punta Bajo (Fig. 3) (Mayer and Vincent, 1999), we speculate that the fault runs to the east offshore north of Punta El Bajo and under the Quaternary volcano (Bigioggero et al., 1988) of Coronado Island. Preliminary work on Carmen Island indicates that it is bounded by north-striking normal faults because flights of 2–4 uplifted marine terraces are exposed within Pliocene marine strata on both sides of the island. Echo-sounder data support the presence of an active graben between Carmen Island and the coast near Loreto (Fig. 12C) (Nava-Sanchez et al., 2001).

Nopolo Subsegment

An anomalous feature of the Loreto segment is the Nopolo area. This ~15-km-long part of the Loreto segment has a major down-to-the-east extensional monocline, but the Nopolo fault has less offset (only 20–30 m) than the Loreto and Escondido faults to its north and south (Fig. 5) (Willsey et al., 2002). The topography of the Nopolo area is distinct within the Loreto segment in that there is a coastal plain that is not bounded by a major fault and the Main Gulf Escarpment is lower, less steep, and wider than in the rest of the Loreto segment (Fig. 6, B and C).

The Nopolo fault aligns with the other main rift-bounding faults, which suggests that it is part of the Loreto segment and not a distinct crustal-scale feature. We explain these anomalies in the Nopolo area as due to major faulting dying out in this area after the protogulf episode (at the end of the Miocene). Thus, the Main Gulf Escarpment was lowered and became less steep by 5–6 m.y. of erosion because it was not maintained by active faulting. This change in the fault activity may have happened because the Pliocene Loreto fault acted as a step in the active fault system from the western boundary of the segment eastward to the offshore faults and in this manner bypassed the Nopolo fault.

Main Gulf Escarpment, Segmentation, and Offshore Faulting

The Loreto to Bahía Concepción region has strong evidence for the existence of two rift segments of ~80–100 km length. Alternating geometry and symmetry of extension are suggested, similar to other continental rifts (Fig. 12). The evidence presented here for the Loreto segment clearly shows that it is bounded by a major fault system on the west that has down-to-the-east offset. The higher relief and steeper and straighter nature of the Main Gulf Escarpment along the Loreto segment compared to the escarpment's nature in the accommodation zones to the north and south coincides spatially with the bounding faults of the Loreto segment. The escarpment is lower and more irregular where rift-bounding faults have been inactive for millions of years or at the accommodation zones between segments. However, the escarpment likely reflects the combined effects of footwall uplift behind the rift-bounding faults and an isostatic response to regional extensional unloading of the Gulf of California during rifting. The ~0.5–2 km of offset on most of the rift-bounding structures (Fig. 5) is too small to account for all of the relief on the escarpment. The escarpment is higher and steeper behind the northern Loreto and Escondido faults, which are the two parts of the segment boundary that remained active into the Quaternary, though at low rates of faulting. This concurrence substantiates the partial role of faulting in developing the escarpment. We suggest that the reason for the relatively modest offset on the rift-bounding faults is that most of the fault activity moved toward the rift center (offshore) after the protogulf stage.

In contrast to the Loreto segment, the Mulegé segment (Axen 1995) has a very different structural and topographic pattern. The major faults are west-dipping normal faults (Wilson, 1948; Johnson et al., 1997), strike-slip faults are not known (cf. McFall, 1968), and Pliocene strata are in small, thin, patches with subhorizontal tilts (Johnson et al., 1997). The Santa Rosalía basin in the northern part of the Mulegé segment has a few hundred meters of east-tilted strata along west-dipping faults (Wilson, 1948). In addition, although the elevation of the Main Gulf Escarpment along the Mulegé segment is high like the Loreto segment, the Mulegé escarpment is consistently more deeply eroded and less steep than the Loreto escarpment (Fig. 6D). All of these characteristics point to a rift segment that is dominated by moderate-sized, west-dipping normal faults without a fault bounding the Main Gulf Escarpment (Axen, 1995).

The nature of segmentation to the south of the Loreto segment is much more problematic and less well understood. Axen (1995) speculated that there was a Timbabichi segment similar to the Mulegé segment. The gently east-dipping strata we observed for ~30 km south of the Loreto segment suggest that this speculation may be correct. However, the Main Gulf Escarpment steps to the east at Bahía Agua Verde (Figs. 2 and 4 and near 25°35′ to 25°40′ in the southeastern corner of Fig. 3), and so the evidence for the nature of the geology of this potential segment is largely along the remote coast south of Bahía Agua Verde and offshore.

Because the rift-bounding faults near Loreto are mainly of modest scale compared to those in many rifts (e.g., Ebinger et al., 1984; Rosendahl, 1987; Colletta et al., 1988; Morley et al., 1990; Chapin and Cather, 1994; Hayward and Ebinger, 1996), an alternative model of dominantly west dipping extension is possible. This model would predict that there will be large-offset, west-dipping faults offshore. Further, in this model, the east-dipping faults and down-to-the-east extensional monoclines of the Loreto segment constitute secondary faults in the hanging wall of the possible larger west-dipping faults. John Fletcher (2001, written commun.) has pointed out that the Loreto segment near Nopolo has some things in common with the Sierra Juárez of northern Baja California, which is demonstrably dominated by west-dipping normal faults (Axen and Fletcher, 1998). Data on offshore faults and basins are clearly required to fully understand the history of the Main Gulf Escarpment and segmentation near Loreto in three dimensions and to develop a more complete view of the strain across the plate margin.

How and Why Does Oblique Rifting Overprint Orthogonal Rifting?

As shown here, the Loreto rift segment is fundamentally a late Miocene (protogulf) feature that was overprinted strongly by transtensional structures with a different extension direction during Pliocene to Quaternary time. The main overprint is represented by the southern Loreto fault and Loreto basin, which formed in the middle of the segment (Fig. 3). The en echelon pattern of left-stepping faults from the northern Loreto fault to the northern monocline is similar to patterns of faulting produced in experiments of oblique rifting (McClay and White, 1995). This correspondence suggests that the northern structures were modified in the transtensional stage. This left-stepping pattern is also present in the late Quaternary fault scarps on the northern Loreto fault (Mayer and Vincent, 1999).

The resulting pattern of faults and topography from the overprinting of transtensional structures is that the footwall of the segment remains a rather simple, unfaulted broad arch that reflects the original segment. The hanging wall of the segment, in contrast, is more complex than hanging walls of many rift segments in orthogonal rifts. The oblique-rift structures cut through the original segment, dividing it up structurally and producing numerous cross-segment topographic highs (Fig. 3). The complex transtensional fault pattern also results in a complex coastal topography with relatively short ranges alternating with narrow coastal plains (Fig. 3). Likewise the pattern of offshore islands does not match the original rift segment. Carmen Island was uplifted in only the southern part of the segment. And the proposed rotation of the island resulted in its north-northeast–south-southwest orientation, which is distinctly different than the north-northwest–south-southeast orientation of the segment boundary. Uncommon synrift volcanic centers create local topographic highs.

The change to an oblique rift occurred because of the jump of the main plate boundary into the Gulf of California at ca. 8–6 Ma. The change near Loreto occurred when most of the rift-bounding faults were abandoned (e.g., the Nopolo down-to-the-east extensional monocline, Willsey et al., 2002), or faulting along them slowed greatly as in the northern Loreto fault (Mayer and Vincent, 1999). The main transtensional Loreto fault cut through the middle of the segment from the rift margin at the northern Loreto fault to offshore. The history of the change to transtension or oblique rifting involved a series of shifts in the location of faulting that generally progressed east toward the center of the rift or to the main plate boundary. This episodic history of change caused a higher portion of the plate motion to be concentrated onto the main plate boundary.

The extension direction in the Loreto segment shifted ~35° clockwise from that of the typical protogulf (east-northeast–west-southwest) direction to the nearly east-west direction of the past few million years. This change did not occur in the La Paz region, where extension in the plate margin continues to be east-northeast–west-southwest today (Fletcher and Munguía, 2000). A thorough analysis of this large variation in structural style along the plate margin is beyond this paper, but we speculate that it is due to differences in strain partitioning.

CONCLUSIONS

This study has conclusions that are germane to the regional geology and evolution of the Gulf of California and for the processes in the formation of rifts in general. The major faults and topography of the Loreto region define the Loreto rift segment, which is 85 km long and has accommodation zones on either end. The segment is bounded on the west by an aligned, but discontinuous, fault system of down-to-the-east normal faults and extensional monoclines that terminate to the north and south. All the rift-bounding faults formed as extensional monoclines and then evolved to normal faults. The footwall of this fault system is the Main Gulf Escarpment, which is broadly arched behind the Loreto segment such that the escarpment is high and steep behind the segment and low and less steep at the accommodation zones. There is an anomalous Nopolo subsegment within the Loreto segment that has a down-to-the-east extensional monocline of moderate offset and a lower and less steep escarpment because faulting died there and moved offshore at the end of the Miocene.

Analysis of secondary faults in the region strongly suggests that there were two stages of deformation related to formation of the Gulf of California. In the middle to late Miocene (protogulf stage), the basic Loreto segment was formed from the rift-bounding monoclines and faults; widespread secondary normal faulting had an east-northeast–west-southwest extension direction (~65°–245°).

The transtensional southern Loreto fault and related structures overprinted the segment in the Pliocene and formed the Loreto basin. These younger structures are mixed normal faults and dextral strike-slip faults. The extension direction rotated clockwise ~35° to ~100°–280°. The locus of the transtensional movements changed numerous times during the Pliocene to Quaternary, and in general, fault activity moved toward the east into the offshore. We speculate that the Loreto fault was linked to a system of normal-slip and strike-slip faults offshore that evolved into the present Alt and Pescadero transform faults. This transition from coastal to offshore faulting occurred in the Pliocene and was accompanied by 35°–40° of clockwise rotation of Carmen Island.

The Mulegé segment (Axen, 1995), north of the Loreto segment, is dominated by west-dipping faults, has a less steep Main Gulf Escarpment, and has no evidence for overprinting by Pliocene to Quaternary deformation. These differences between Mulegé and Loreto suggest a pattern of adjacent segments with alternating geometry and symmetry of faults (Axen, 1995) as seen in many other rifts. The region south of the Loreto segment is not well known, but the La Paz region has a very different style of faulting (e.g., Fletcher et al., 2000; Fletcher and Munguía, 2000); thus, there must be a major change in the pattern of segmentation between the Loreto segment and La Paz.

The history of the plate margin near Loreto has several implications for interpretation of processes that generally occur in oblique-divergent plate boundaries. (1) Our data suggest that structural segmentation is widespread along Baja California, as Axen (1995) speculated. The Loreto region further suggests that there may be a pattern of alternating vergence in the segmentation, though more data are required from the offshore gulf to verify this pattern. We have also documented that the segmentation is manifested in a predictable topographic signature. (2) There is a general episodic development of the plate boundary with a progressive concentration of plate motion onto the main boundary. This history is broadly similar to the changes in the Afar rift system where fault activity is also moving toward the center of the rift (Hayward and Ebinger, 1996). (3) The role of the Loreto fault as the main transtensional structure along the margin suggests that it played an integral part in the initiation of the transform faults. The suggestion from the Loreto region is that one method of initiating transform faults in an oblique-divergent plate boundary is by development of a series of en echelon strike-slip faults, some of which extend from the boundary of the rift. For a short period of time (<1 m.y.), these strike-slip faults move at rates that are a large part of the total relative plate motion. The en echelon strike-slip faults rapidly evolve into a series of true transform faults and short spreading ridges. (4) Our data from the Loreto segment show that despite a significant decrease of fault activity within the plate margin since the Pliocene, the margin was still subject to discontinuous normal faulting in the late Quaternary. This finding means that faulting of a rifting style has continued for at least 2 m.y. after the modern transform–spreading-ridge system formed (also see Fletcher and Munguía, 2000, for similar results). Thus, the rift-to-drift transition is not as abrupt as commonly thought.

ACKNOWLEDGMENTS

This research was supported by National Science Foundation grants EAR9526506 and EAR9802792. We thank the participants of the Penrose Conference held in Loreto in 1996 for numerous constructive comments on our research. We thank in particular former students Andy Stone, Peter Falk, and Shawn Willsey, and colleagues Jorge Ledesma, Markes Johnson, John Fletcher, Gary Axen, Joann Stock, Arturo Martín, and Chris Henry for discussions. We also thank Gary Axen, Cindy Ebinger, John Fletcher, Gary Karner, Bob Bohannon, David Scholl, Scott Paterson, and Joann Stock for constructive reviews that considerably sharpened the manuscript.

REFERENCES CITED

Angelier, J., Colletta, B., Chorowicz, J., Ortlieb, L., and Rangin, C., 1981, Fault tectonics of the Baja California Peninsula and the opening of the Sea of Cortez, Mexico: Journal of Structural Geology, v. 3, p. 347–357.

Atwater, T., and Stock, J., 1998, Pacific–North America plate tectonics of the Neogene southwestern United States: An update: International Geology Review, v. 40, p. 375–402.

Axen, G., 1995, Extensional segmentation of the Main Gulf Escarpment, Mexico and United States: Geology, v. 23, p. 515–518.

Axen, G.J., and Fletcher, J.M., 1998, Late Miocene–Pleistocene extensional faulting, northern Gulf of California, Mexico and Salton Trough, California: International Geology Review, v. 40, p. 217–244.

Bigioggero, B., Capaldi, G., Chiesa, S., Montrasio, A., Vezzoli, L., and Zanchi, A., 1988, Postsubduction magmatism in the Gulf of California: The Isla Coronados (Baja California Sur, Mexico): Istituto Lombardo Accademia di Scienze e Lettere (Rendiconti Scienze B), v. 121, p. 117–132.

Bigioggero, B., Chiesa, S., Zanchi, A., Montrasio, A., and Vezzoli, L., 1995, The Cerro Mencenares volcanic center, Baja California Sur: Source and tectonic control on postsubduction magmatism with the Gulf rift: Geological Society of America Bulletin, v. 107, p. 1108–1122.

Bosworth, W.R., 1985, Geometry of propagating rifts: Nature, v. 316, p. 625–627.

Braun, J., and Beaumont, C., 1989, A physical explanation of the relation between flank uplifts and the breakup unconformity at rifted continental margins: Geology, v. 17, p. 760–764.

Buck, W.R., 1988, Flexural rotation of normal faults: Tectonics, v. 7, p. 959–973.

Chapin, C.E., and Cather, S.M., 1994, Tectonic setting of the axial basins of the northern and central Rio Grande rift, *in* Keller, G.R., and Cather, S.M., eds., Basins of the Rio Grande rift: Structure, stratigraphy, and tectonic setting: Geological Society of America Special Paper 291, p. 5–26.

Colletta, B., Le Quellec, P., Letouzy, J., and Moretti, I., 1988, Longitudinal evolution of the Suez rift structure (Egypt): Tectonophysics, v. 153, p. 221–233.

Crossley, R., and Crow, M.J., 1980, The Malawi rift, *in* Geodynamic evolution of the Afro-Arabian rift system: Accademia Nationale Lincei, p. 77–87.

Dixon, T., Farina, F., DeMets, C., Suarez Vidal, F., Fletcher, J., Marquez-Azua, B., Miller, M., and Umhoefer, P., 2000, New kinematic models for Pacific–North America motion from 3 Ma to present: Evidence for a ''Baja California shear zone'': Geophysical Research Letters, v. 27, p. 3961–3964.

Dorsey, R.J., and Umhoefer, P.J., 2000, Tectonic and eustatic controls on sequence stratigraphy of the Pliocene Loreto basin, Mexico: Geological Society of America Bulletin, v. 112, p. 177–199.

Dorsey, R.J., Umhoefer, P.J., and Renne, P., 1995, Rapid subsidence and stacked Gilbert-type fan deltas, Pliocene Loreto basin, Baja California Sur, Mexico: Sedimentary Geology, v. 98, p. 181–204.

Ebinger, C.J., 1989a, Geometric and kinematic development of border faults and accommodation zones, Kivu-Rusizi rift, Africa: Tectonics, v. 8, p. 117–133.

Ebinger, C.J., 1989b, Tectonic development of the western branch of the East Africa rift system: Geological Society of America Bulletin, v. 101, p. 885–903.

Ebinger, C.J., Crow, M.J., Rosendahl, B.R., Livingstone, D.L., and LeFournier, J., 1984, Structural evolution of Lake Malawi, Africa: Nature, v. 308, p. 627–629.

Fantozzi, P.L., 1996, Transition from continental to oceanic rifting in the Gulf of Aden: Structural evidence from field mapping in Somalia and Yemen: Tectonophysics, v. 259, p. 285–311.

Faulds, J.E., and Varga, R.J., 1998, The role of accommodation zones and transfer zones in the regional segmentation of extended terranes, *in* Faulds, J.E., and Stewart, J.H., eds., Accommodation zones and transfer zones: The regional segmentation of the Basin and Range povince: Geological Society of America Special Paper 323, p. 1–47.

Fletcher, J.M., and Munguía, L., 2000, Active continental rifting in southern Baja California, Mexico: Implications for plate motion partitioning and the transition to sea floor spreading: Tectonics, v. 19, p. 1107–1123.

Fletcher, J.M., Kohn, B.P., Gleadow, A.J.W., and Foster, D.A., 2000, Heterogeneous cooling and exhumation of the Los Cabos block, southern Baja California: Evidence from fission-track thermochronology: Geology, v. 28, p. 107–110.

Gastil, R.G., Phillips, R.P., and Allison, E.C., 1975, Reconnaissance geology of the state of Baja California: Geological Society of America Memoir 140, 170 p.

Gawthorpe, R.L., and Hurst, J.M., 1993, Transfer zones in extensional basins; their structural style and influence on drainage development and stratigraphy: Journal of the Geological Society of London, v. 150, p. 1137–1152.

Goff, J.A., Bergman, E.A., and Solomon, S.C., 1987, Earthquake source mechanisms and transform fault tectonics in the Gulf of California: Journal of Geophysical Research, v. 92, p. 10485–10510.

Hausback, B.P., 1984, Cenozoic volcanic and tectonic evolution of Baja California, Mexico, *in* Frizzell, V.A., ed., Geology of the Baja California Peninsula: Bakersfield, California, Pacific Section, Society of Economic Paleontologists and Mineralogists, p. 219–236.

Hayward, N.J., and Ebinger, C.J., 1996, Variations in the along-axis segmentation of the Afar rft system: Tectonics, v. 15, p. 244–257.

Henry, C.D., 1989, Late Cenozoic Basin and Range structure in western Mexico adjacent to the Gulf of California: Geological Society of America Bulletin, v. 101, p. 1147–1156.

Holt, J.W., Holt, E.W., and Stock, J.M., 2000, An age constraint on Gulf of California rifting from the Santa Rosalía basin, Baja California Sur, Mexico: Geological Society of America Bulletin, v. 112, p. 540–549.

Humphreys, E.D., and Weldon, R.J., II, 1991, Kinematic constraints on the rifting of Baja California, *in* Dauphin, J.P., and Simoneit, B.R.T., eds., The Gulf and Peninsula province of the Californias: American Association of Petroleum Geologists Memoir 47, p. 217–229.
Jackson, J.A., and White, N.J., 1989, Normal faulting in the upper continental crust: Observations from regions of active extension: Journal of Structural Geology, v. 11, p. 15–36.
Johnson, M.E., Ledesma-Vázquez, J., Mayall, M.A., and Minch, J., 1997, Upper Pliocene stratigraphy and depositional systems: The Peninsula Concepción basins in Baja California Sur, Mexico, *in* Johnson, M.E., and Ledesma-Vázquez, J., eds., Pliocene carbonates and related facies flanking the Gulf of California, Baja California, Mexico: Geological Society of America Special Paper 318, p. 57–72.
Karig, D.E., and Jensky, W., 1972, The proto–Gulf of California: Earth and Planetary Science Letters, v. 17, p. 169–174.
Lewis, C.J., and Baldridge, W.S., 1994, Crustal extension in the Rio Grande rift, New Mexico: Half-grabens, accommodation zones, and shoulder uplifts in the Ladron Peak–Sierra Lucero area, *in* Keller, G.R., and Cather, S.M., eds., Basins of the Rio Grande rift: Structure, stratigraphy, and tectonic setting: Geological Society of America Special Paper 291, p. 135–155.
Lister, G.S., Etheridge, M.A., and Symonds, P.A., 1986, Detachment faulting and the evolution of passive continental margins: Geology, v. 14, p. 246–250.
Lonsdale, P., 1989, Geology and tectonic history of the Gulf of California, *in* Winterer, E.L., et al., eds., The eastern Pacific Ocean and Hawaii: Boulder, Colorado, Geological Society of America, Geology of North America, v. N, p. 499–521.
Lyle, M., and Ness, G.E., 1991, The opening of the Gulf of California, *in* Dauphin, J.P., and Simoneit, B.R.T., eds., The Gulf and Peninsula province of the Californias: American Association of Petroleum Geologists Memoir 47, p. 403–423.
Mack, G.H., and Seager, W.R., 1995, Transfer zones in the southern Rio Grande rift: Journal of the Geological Society [London], v. 152, p. 551–560.
Marrett, R., and Allmendinger, R.W., 1990, Kinematic analysis of fault-slip data: Journal of Structural Geology, v. 12, p. 973–986.
Martín-Barajas, A., Stock, J.M., Layer, P., Hausback, B., Renne, P., and López-Martínez, M., 1995, Arc-rift transition volcanism in the Puertecitos volcanic province, northeastern Baja California, Mexico: Geological Society of America Bulletin, v. 107, p. 407–424.
Mayer, L., and Vincent, K.R., 1999, Active tectonics of the Loreto area, Baja California Sur, Mexico: Geomorphology, v. 27, p. 243–255.
McClay, K.R., and Ellis, P.G., 1987, Geometry of extensional fault systems developed in model experiments: Geology, v. 15, p. 341–344.
McClay, K.R., and White, M.J., 1995, Analogue modelling of orthogonal and oblique rifting: Marine and Petroleum Geology, v. 12, p. 137–151.
McFall, C.C., 1968, Reconnaissance geology of the Concepcíon Bay area, Baja California, Mexico: Stanford University Publications in Geological Sciences, v. 10, p. 1–25.
McLean, H., 1988, Reconnaissance geologic map of the Loreto and part of the San Javier Quadrangles, Baja California Sur, Mexico: U.S. Geological Survey Map MF-2000, scale 1:50 000.
Moore, D.G., and Buffington, E.C., 1968, Transform faulting and growth of the Gulf of California since the late Pliocene: Science, v. 161, p. 1238–1241.
Morley, C.K., Nelson, R.A., Patton, T.L., and Munn, S.G., 1990, Transfer zones in the East Africa rift system and their relevance to hydrocarbon exploration in rifts: American Association of Petroleum Geologists Bulletin, v. 74, p. 1234–1253.
Nava-Sanchez, E.H., Gorsline, D.S., and Molina-Cruz, A., 2001, The Baja California peninsula borderland: Structural and sedimentological characteristics: Sedimentary Geology, v. 144, p. 63–82.
Ness, G.E., and Lyle, M.W., 1991, A seismo-tectonic map of the Gulf and Peninsula province of the Californias, in Dauphin, J.P., and Simoneit, B.R.T., eds., The Gulf and Peninsula province of the Californias: American Association of Petroleum Geologists Memoir 47, p. 403–423.
Rosendahl, B.R., 1987, Architecture of continental rifts with special reference to East Africa: Annual Review of Earth and Planetary Science, v. 15, p. 445–503.
Rosendahl, B.R., Reynolds, D.J., Lorber, P.M., Burgess, C.F., McGill, J., Scott, D., Lambiase, J.J., and Derkson, S.J., 1986, Structural expressions of rifting: Lessons from Lake Tanganyika, Africa, *in* Frostick, L.E., Renaut, R.W., Reid, I., and Tiercelin, J.J., eds., Sedimentation in the African rifts: Geological Society of London Special Publication 25, p. 29–43.
Royden, L., and Keen, C.E., 1980, Rifting processes and thermal evolution of the continental margin of eastern Canada determined from subsidence curves: Earth and Planetary Science Letters, v. 51, p. 343–361.
Sawlan, M.G., 1991, Magmatic evolution of the Gulf of California rift, *in* Dauphin, J.P., and Simoneit, B.R.T., eds., The Gulf and Peninsula province of the Californias: American Association of Petroleum Geologists Memoir 47, p. 217–229.
Sawlan, M.G., and Smith, J.G., 1984, Petrologic characteristics, age, and tectonic setting of Neogene volcanic rocks in northern Baja California Sur, Mexico, *in* Frizzell, V.F., ed., Geology of the Baja California Peninsula: Los Angeles, SEPM Pacific Section Field Trip Guidebook, v. 39, p. 237–251.
Scholz, C.H., and Contreras, J.C., 1998, Mechanics of continental architecture: Geology, v. 26, p. 967–970.
Serpa, L., and Pavlis, T., 1996, Three dimensional model for the late Cenozoic history of the Death Valley region, southeastern California: Tectonics, v. 15, p. 1113–1128.
Smith, J.T., 1991, Cenozoic marine mollusks and paleogeography of the Gulf of California, *in* Dauphin, J.P., and Simoneit, B.R.T., eds., The Gulf and Peninsula province of the Californias: American Association of Petroleum Geologists Memoir 47, p. 637–666.
Spencer, J.E., and Normark, W.R., 1979, Tosco-Abreojos fault zone: A Neogene transform plate boundary within the Pacific margin of southern Baja California, Mexico: Geology, v. 7, p. 554–557.
Steckler, M.S., 1985, Uplift and extension of the Gulf of Suez: Indications of induced mantle convection: Nature, v. 317, p. 135–139.
Stock, J.M., and Hodges, K.V., 1989, Pre-Pliocene extension around the Gulf of California and the transfer of Baja California to the Pacific plate: Tectonics, v. 8, p. 99–115.
Stock, J.M., and Lee, J., 1994, Do microplates in subduction zones leave a geological record?: Tectonics, v. 13, p. 1472–1487.
Stock, J.M., and Molnar, P., 1988, Uncertainties and implications of the Late Cretaceous and Tertiary position of North America relative to the Farallon, Kula, and Pacific plates: Tectonics, v. 7, p. 1339–1384.
Suarez-Vidal, F., Armijo, R., Morgan, G., Bodin, P., and Gastil, R.G., 1991, Framework of recent and active faulting in northern Baja California, *in* Dauphin, J.P., and Simoneit, B.R.T., eds., The Gulf and Peninsula province of the Californias: American Association of Petroleum Geologists Memoir 47, p. 285–300.
Tamsett, D., 1984, Comments of the development of rifts and transform faults during continental breakup; examples from the Gulf of Aden and northern Red Sea: Tectonophysics, v. 104, p. 35–46.
Umhoefer, P.J., and Stone, K.A., 1996, Description and kinematics of the southeast Loreto basin fault array, Baja California Sur, Mexico: A positive field test of oblique-rift models: Journal of Structural Geology, v. 18, p. 595–614.
Umhoefer, P.J., Dorsey, R.J., and Renne, P., 1994, Tectonics of the Pliocene Loreto basin, Baja California Sur, Mexico, and the evolution of the Gulf of California: Geology, v. 22, p. 649–652.
Umhoefer, P.J., Dorsey, R.J., Willsey, S., Mayer, L., and Renne, P., 2001, Stratigraphy and geochronology of the Comondú Group near Loreto, Baja California Sur, Mexico: Sedimentary Geology, v. 144, p. 125–147.
Upcott, N.M., Mukasa, R.K., Ebinger, C.J., and Karner, G.D., 1996, Along-axis segmentation and isostasy in the western rift, East Africa: Journal of Geophysical Research, v. 101, p. 3247–3268.
Weissel, J.K., and Karner, G.D., 1989, Flexural uplift and rift flanks due to mechanical unloading of the lithosphere during extension: Journal of Geophysical Research, v. 94, p. 13919–13950.
Wernicke, B., and Axen, G.J., 1988, On the role of isostasy in the evolution of normal fault systems: Geology, v. 16, p. 848–851.
Willsey, S.P., Umhoefer, P.J., and Hilley, G.E., 2002, Early evolution of an extensional monocline by a propagating normal fault: 3-D analysis from combined field study and numerical modeling: Journal of Structural Geology, v. 24, p. 651–669.
Wilson, I.F., 1948, Buried topography, initial structures, and sedimentation in Santa Rosalía area, Baja California, Mexico: American Association of Petroleum Geologists Bulletin, v. 32, p. 1762–1807.
Wilson, I.F., and Rocha, V.S., 1955, Geology and mineral deposits of the Boleo copper district, Baja California, Mexico: U.S. Geological Survey Professional Paper 273, p. 1–134.
Zanchi, A., 1994, The opening of the Gulf of California near Loreto, Baja California, Mexico: From basin and range extension to transtensional tectonics: Journal of Structural Geology, v. 16, p. 1619–1639.

MANUSCRIPT RECEIVED BY THE SOCIETY OCTOBER 4, 2000
REVISED MANUSCRIPT RECEIVED DECEMBER 13, 2001
MANUSCRIPT ACCEPTED DECEMBER 18, 2001

Printed in the USA